Available online at www.sciencedirect.com
ScienceDirect
International Journal of Coal Geology 71 (2007) 129–152
International Journal of COAL GEOLOGY
www.elsevier.com/locate/ijcoalgeo

Concentration and distribution of trace elements in lignite from the Shengli Coalfield, Inner Mongolia, China: Implications on origin of the associated Wulantuga Germanium Deposit

Huawen Qi [a,*], Ruizhong Hu [a], Qi Zhang [a,b]

[a] *State Key laboratory of Ore Deposit Geochemistry, Institute of Geochemistry, Chinese Academy of Sciences, Guiyang 550002, China*
[b] *Graduate School, Chinese Academy of Sciences, Beijing 100039, China*

Received 30 May 2006; received in revised form 9 August 2006; accepted 9 August 2006
Available online 25 September 2006

Abstract

The Wulantuga Germanium Deposit (WGD), hosted in coal seams with Ge resources up to 1600 Mt, is located in the Shengli Coalfield in Xilingol, Inner Mongolia, China. Forty-two channel samples of Ge-bearing lignites of the No.6-1 coal seam in Lower Cretaceous Bayanhua Formation were collected and analyzed by inductively coupled plasma mass spectrometry (ICP-MS). The mode of occurrence of elements in selected lignite samples were studied by cluster analysis and scanning electron microscope with energy-dispersive X-ray spectrometer (SEM-EDX). The lignite samples of WGD are distinctly enriched in Be, Ge, Sb, W, and U and depleted in Rb, Nb, Sn, and Ta, compared with the average composition of upper continental crust. The average concentrations of above enriched elements also are higher than those of overlying sandstone of WGD and contemporary Ge-barren lignite of Hongqi Coal Mine in Shenli Coalfield, as well as the average concentration of elements in the USA coals and worldwide coals. With an exception of Sr, most trace elements and ash yields obey the log normal distribution in all 42 lignite samples collected from WGD. The elements in these lignites may be classified into four groups: The first group (Ge–Mo association) contains elements with negative correlation coefficients with ash yields, and they show mainly organic affinity. The elements in the second group (Tl–Ga–Zn–Co association) show negative to moderate correlation coefficients with ash yields, and may also have an organic affinity, but most of them are mainly related to mineral matter (such as sphalerite). The last two groups (Rb–Cs and W–U–Cd–Y–Pb–Cu–Hf–Zr–Th–Sn–Nb–Ta–TiO_2–Sb–Ba–Sr–MnO–Be associations) contain elements with moderate to high correlation coefficients with ash yields, much of them associated mainly with mineral matter (such as anatase, manganite, zircon, and barite) as identified by SEM-EDX analysis, and show mainly aluminosilicate affinity. Silver-bearing particles or native silver were identified by SEM-EDX in the lignites from WGD and Hongqi Coal Mine. Germanium and Mo can concentrate in different proportion of coal seam in different sections, while other elements more or less follow the distribution of ash yield. The TiO_2-normalized elemental profiles reveal that Be/TiO_2, Ge/TiO_2, W/TiO_2, U/TiO_2, Mo/TiO_2, Sb/TiO_2, Tl/TiO_2, and Sr/TiO_2 ratios of the lignite samples in three sections of WGD are generally one or two order of magnitude higher than the reference ratios of sandstone from WGD and lignite from Hongqi Coal Mine, much (more than 90%) of these elements (Be, Ge, W, U, Mo, Sb, Tl, and Sr) may be transported into coal seam by solution. The Ge-bearing lignites from WGD are distinctly characterized by lower Rb/Cs ratios, higher U/Th ratios, different from those of the overlying sandstone from WGD and contemporary lignite from Hongqi Coal Mine. Most trace elements in the Ge-bearing lignite of WGD may have been derived from a granitic source, and the enrichment of Be,

* Corresponding author.
E-mail address: qihuawen@vip.gyig.ac.cn (H. Qi).

0166-5162/$ - see front matter
doi:10.1016/j.coal.2006.08.005

Ge, Sb, W, and U may be attributed to an epigenetic lateral transferred Ge-bearing solution that leached these elements from the granitic source and transported them into the lignite.

Keywords: Lignite; Trace element; Wulantuga Germanium Deposit; Shengli Coalfield; Inner Mongolia; China

1. Introduction

Few elements in coal have attracted as much attention as germanium (Ge), not only because Ge has the highest organic affinities of all elements in coal, but also because of the possibility of Ge utilization as by-product in process of the combustion of Ge-rich coals (Seredin and Danilcheva, 2001; Seredin, 2006). There is abundant literature on Ge occurrence in coal (Weber, 1973; Smimov, 1977; Bouška, 1981; Valkovic, 1983; Bernstein, 1985; Hower et al., 2002; Yudovich, 2003; and the references therein). However, coal-hosted Ge deposits, with unusual reserves >1000 Mt and concentration up to 3000 ppm were reported from three areas: Russian Far East (Seredin and Danilcheva, 2001); the Lincang Ge Deposit, Western Yunnan of China (Zhuang et al., 1998; Qi et al., 2004); and the Wulantuga Ge Deposit, Inner Mongolia, China (Wang, 1999; Qing, 2001; Du et al., 2003, 2004; Zhuang et al., 2006).

The Wulantuga Germanium Deposit (WGD), discovered by the Inner Mongolia Coalfield Geology Bureau at Xilinhaote, Inner Mongolia in 1998, is a paragenetic coal/Ge deposit, which was also named 'the paragenetic germanium deposit in Shenli Coalfield' in some Chinese literatures (such as Du et al., 2003, 2004). The Ge contained in the deposit is estimated to be up to 1600 Mt, accounting for 30% of China's Ge reserves (Brown, 2000). Wang (1999) and Qing (2001) stated the geological characteristics and exploration of the deposit. Du et al. (2003, 2004) discussed Ge content variation regularity and the relationship between Ge concentration and volatile matter, ash yield and sulfur content in the lignite samples of the No.6-1 coal seam collected from different boreholes. A preliminary study of geochemistry and mineralogy of 12 coal samples from this deposit were conducted by Zhuang et al. (2006).

The geological distribution of Ge contents in the coal seam of WGD are quite different from those of the Lincang Ge Deposit (LGD) (Qi et al., 2004), and Ge deposits (such as Bikin, Pavlovka, Rakovka, and Shkotovo) in the Russian Far East (GDRFE) (Seredin and Danilcheva, 2001), and the genetic mechanism of the WGD needs to be studied. Open pit minning operations are active in Wulantuga, providing an excellent site for detailed sampling and an ideal case for examining the mechanism of Ge enrichment. In this paper, we discussed the trace element geochemistry of 42 lignite samples from WGD. The aim of this study is: (1) to reveal the geochemical variation of different elements, especially of Ge, in the metallogenic lignite, (2) to find the possible link between Ge and other elements, and (3) to discuss the possible source and genetic model of Ge enrichment in the metallogenic lignite of this area.

2. Geological setting

The Shengli Coalfield is located in Wunite Hollow, the western part of Daxinanling Mountain and the eastern part of Erlian Basin Groups, is 45-km wide (W–E) and 76-km long (N–S), and has a total area of 342 km^2. The main structure in the coalfield is a wide and flat syncline with a NE to SW direction, and the main strata are the Lower Cretaceous Bayanhua Formation (Du et al., 2003).

Lower Cretaceous Bayanhua Formation, consisting of Tenggeer and Saihantala Groups and deposited in the Neocathaysian rift basin, was a set of continental coal-bearing sequence, with a thickness more than 1 km. There are 15 coal seams in the upper portion of Tenggeer Group and the lower portion of Saihantala Group. The No.6-1 coal seam in the lower portion of Saihantala Group is the main coal seam in the Shenli Coalfield (42% of the coal reserves of the coalfield), with a thickness ranging from 0.82 m to 123.8 m (33.09 m on average). The Shengli coal is a medium ash coal, with relatively low sulfur content and a subbituminous rank (Zhuang et al., 2006). The overlying strata consist mainly of sandstone and conglomerate, and the underlying strata consist mainly of dark mudstone, siltstone, and the No.6-2 coal seam in local places (Du et al., 2003).

The Wulantuga Ge Deposit is situated on the southwestern margin of Shengli Coalfield (Fig. 1), limited to an area of 0.72 km^2 of the No.6-1 coal seam. Ge mineralization occurs in the No.6-1 coal seam. The minefield consist of monocline strata that dip 5–15° N. The thickness of the No.6-1 coal seam varies from 0.82 to 16.66 m (9.88 m on average), and gradually increases from the outcrop of the No.6-1 coal seam in the southern part to the northern part of mined area. The structure of this coal seam is quite simple, only one thin (0.15 m–0.30 m) carboniferous mudstone bench and five thin

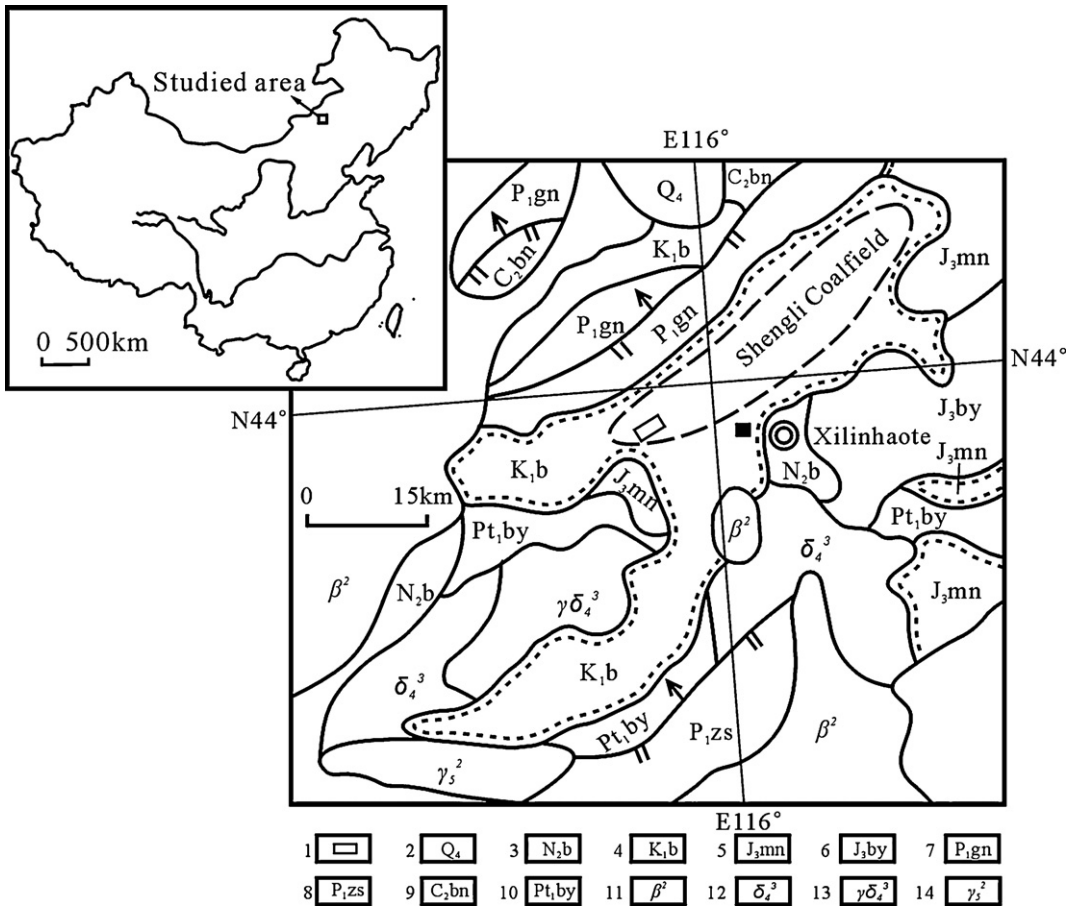

Fig. 1. The sketched regional geological map of Wulantuga Germanium Deposit (modified after Wang, 1999). 1. Wulantuga Germanium Deposit 2. Holocene 3. Neogene Baogedawula Group 4. Lower Cretaceous Baiyanhua Group 5. Upper Jurassic Manitu Group 6. Upper Jurassic Baiyingaolao Group 7. Lower Permian Gegenaobao Group 8. Lower Permian Zhesi Group 9. Upper Carboniferous Benbatu Group 10. Lower Proterozoic Baoyintu Group 11. Quaternary Basalt 12. Hercynian Diorite 13. Hercynian Granodiorite 14. Late Jurassic Granite. The solid black square stands for Hongqi Coal Mine.

(<5 cm) clay partings distributed in the lower and upper portions, respectively. This coal seam is characterized by a relatively high ash yield (21% db on average, $n=12$), relatively low calorific value (23.85 MJ/kg on average, $n=12$), low sulfur content (1% db on average, $n=12$), high vitrinite (54–98%), and low to medium inertinite (b1–30%) and liptinite (2–17.5%) contents (Zhuang et al., 2006).

The Ge ore-bodies, basically accordant with the No.6-1 coal seam, were delineated by Ge content ≥30 ppm (whole coal basis) in the 1–5-m long samples collected from 34 boreholes (Wang, 1999; Du et al., 2003). In the study area, the southern and the northern extending part of the No.6-1 coal seam contain relatively higher Ge than the eastern and western part (Fig. 2). In cross section, prospecting data show Ge content in the No.6-1 coal seam ranging from 138 to 820 ppm (244 ppm on average, whole coal basis, Wang, 1999), and Ge enriched simultaneously in the top, bottom, and (or) the middle portions of the No.6-1 coal seam, depending on different locations of boreholes (Du et al., 2003; Fig. 3). The majority of bore data show a peak of Ge content in the middle proportion of the No.6-1 coal seam (Du et al., 2003). The No.6-2 coal seam, which is 4–11.56-m below the No.6-1 coal seam, contains 10 to 110 ppm Ge (26.8 ppm on average, whole coal basis). The roof and floor rocks contain 2.1–13 ppm Ge (7 ppm on average) (Wang, 1999).

There are two NNW-striking faults that dip 70–75° to NE in the western and eastern margin of the minefield (Fig. 2). These two faults interrupt the continuous distribution of the No.6-1 coal seam. The west fault (F_1), with an offset of 20–50 m, exposed the No.6-1 coal seam in the footwall, while the east fault (F_2), with an

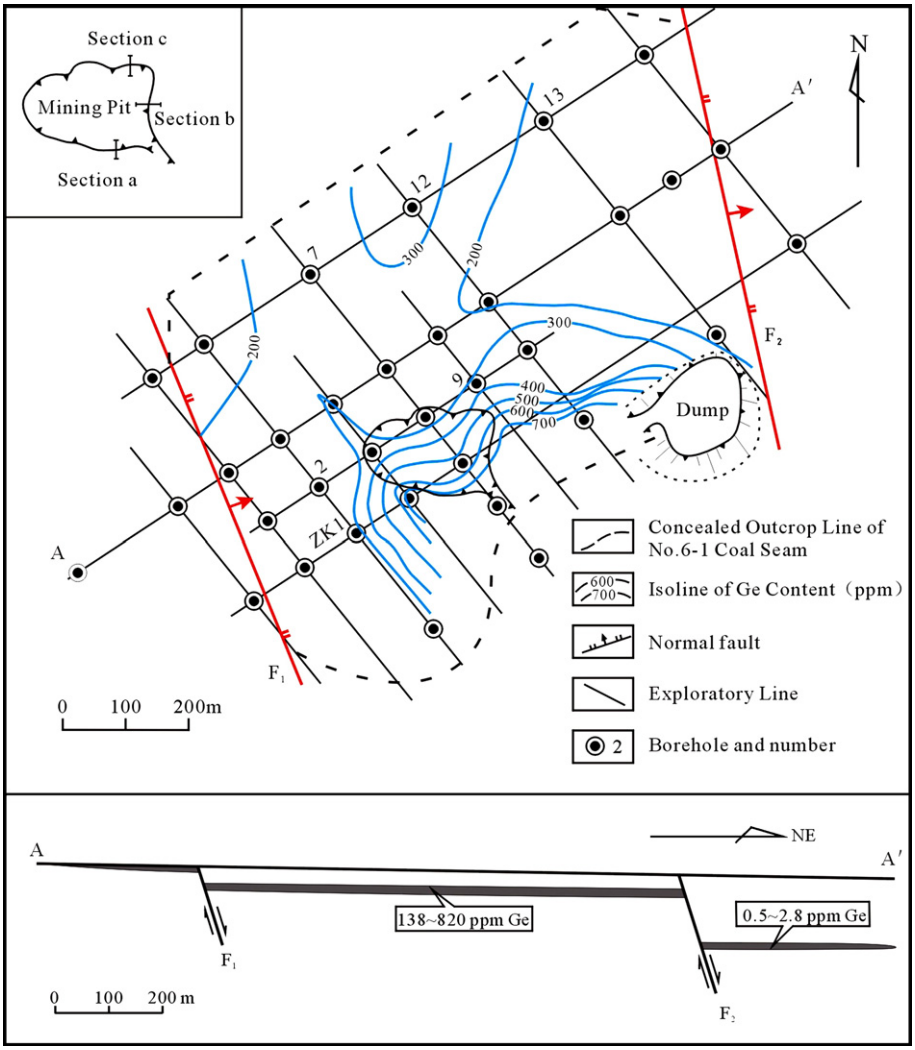

Fig. 2. Isopach map of Ge content in lignite from the Wulantuga Germanium Deposit (modified after Wang, 1999). The small fig on the top left corner show the special distribution of three sampling sections, while the sketch fig on the bottom show the distribution of No.6-1 coal seam along NE direction.

offset of 90–110 m, deeply buried the No.6-1 coal seam in the hanging wall. The borehole data show that the depth of the No.6-1 coal seam in the hanging wall of the east fault is up to 100 m, and Ge content in the coal seam ranges from 0.5 to 2.8 ppm (whole coal basis, Wang, 1999).

3. Sampling and analytical methods

A total of 42 channel samples of lignite were collected from the recent strip-mine benches of the No.6-1 coal seam at different locations within the mine. Among the whole samples, 29 0.15-m wide × 0.20-m long × 0.10-m deep samples were sampled from the top downwards in the coal seam at three different sections (section a, b and c in Fig. 2), with an interval of 20–100 cm, while the other samples were randomly collected from different parts of the coal seam. The distances between the three sections are less than 80 m. The bottom of the No.6-1 coal seam is still unmined and buried, so no samples were collected from it. Two samples of sandstone from the overlying strata of the No.6-1 coal seam in WGD mine and three samples of lignite from the No.6-1 coal seam in the Hongqi Coal Mine, without Ge mineralization, also were collected for comparison.

All the samples were ground and passed through a 75 μm sieve, and dried at 105 °C for 4 h. After drying, a 50 mg sample was placed in a PTFE pressure bomb. To each sample, we added 1 ml analytical reagent-grade HF

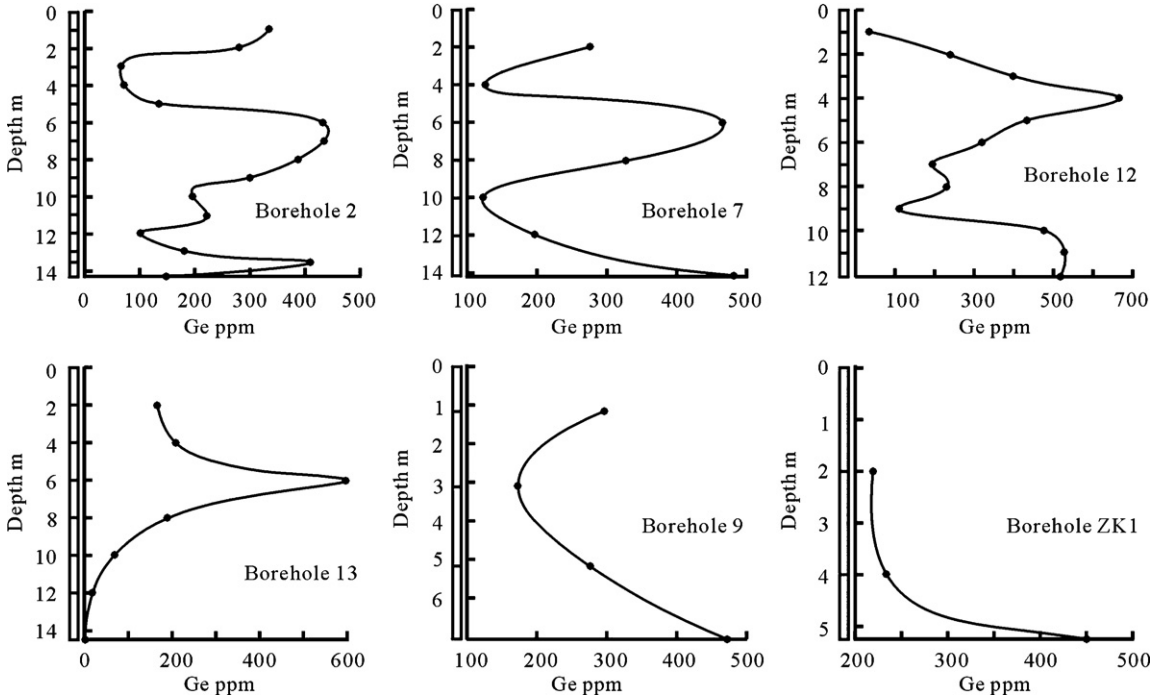

Fig. 3. Vertical distribution of Ge in lignite seam from selected representative boreholes (modified after Du et al., 2004). The blank bars represent the length of collected samples.

and 3 ml analytical reagent-grade HNO_3, then the sealed bomb was heated to 195 °C for 48 h to nitrify the sample. After that, the sample within the PTFE bomb was distilled to dryness to remove Si and residual HF, then 2 ml analytical reagent-grade HNO_3 was added into the bomb, and the sample was re-nitrified at 130 °C for 10 h. After cooling, 500 ng Rh was added into the solution as an internal standard. The final solution reached 50 ml by addition of the distilled deionized water. In order to protect the ICP-MS, a 1 ml solution of each sample was separated and diluted to 4 ml by addition of 4% HNO_3. Then the samples were determined directly by a PE Elan 6000 ICP-MS in Guangzhou Institute of Geochemistry, Chinese Academy of Sciences. Digestion and analysis of international reference material GSR-1 was prepared following the same procedures. Each sample was analyzed five times, and the average count was used to calculate the content of 26 trace elements in the sample. Analytical errors were estimated less than 8% for most of trace elements.

The modes of occurrence of some elements in selected lignite samples were investigated by means of a JSM 6460 LV scanning electron microscope with energy-dispersive X-ray spectrometer (SEM-EDX) in the Institute of Geochemistry, Chinese Academy of Sciences. The ground samples were placed on electric NEM tape, and then their mineral phases were observed in backscattered electron mode and the elemental composition determined by EDX. The organic/inorganic affinity of different elements also were studied using the correlation of elements with 900 °C ash yields. An element is generally considered organically bound if its concentration maintains almost the same level or decreases with increasing ash content, but it is considered inorganically bound if its concentration in coal increases with increasing ash content (Goodarzi, 1988; Foscolos et al., 1989; Krotenski and Sotirov, 2002).

4. Results and discussions

4.1. Contents and enrichment factor of trace element in lignite

The lignite samples from WGD are distinctly enriched in Be, Ge, Sb, W, and U, and depleted in Rb, Nb, Sn, and Ta, compared with the average composition of upper continental crust (Taylor and McLennan, 1985) (Table 1; Fig. 4a–d). The average concentrations of Tl, U, Be, W, Ge, and Sb are 9.14–386 times higher than those of upper continental crust. Strontium, Zn, Co, Cs, Cd, and Mo have average concentrations a little more than those of upper continental crust (from 1.16 to 4.17

Table 1
Trace element compositions (ppm) and ash yields of lignites (%) from the Wulantuga Germanium Deposit

	WL-1	WL-2	WL-3	WL-4	WL-5	WL-6	WL-7	WL-8	WL-9	WL-10	WL-11	WL-12	WL-13	WL-14	WL-15
Be	78.1	42.7	53.8	92.8	111	81.8	54.1	64.6	27.3	32.5	24.3	15.2	8.94	68.8	80.4
TiO_2	1681	1656	658	2923	3309	2405	3394	636	1181	340	863	731	298	1468	666
MnO	125	82.3	114	191	180	191	144	148	179	85.8	74.2	56.7	48.6	154	127
Co	17.5	8.92	14.7	21.0	20.6	20.2	16.3	15.0	12.7	5.26	3.80	2.46	2.28	24.5	35.4
Cu	20.8	14.4	9.97	25.1	26.5	23.0	26.4	12.1	9.74	4.67	9.94	8.31	8.32	19.3	9.81
Zn	118	107	88.7	207	180	205	149	106	60.0	13.0	9.60	87.0	4.64	424	393
Ga	16.1	1.96	3.38	11.2	12.7	6.59	8.88	3.07	3.66	1.31	3.16	1.01	0.48	3.22	2.81
Ge	133	31.4	53.4	288	179	30.9	52.8	41.9	68.5	88.6	152	672	1424	27.0	43.7
Rb	4.34	3.80	1.85	16.0	8.07	9.09	28.0	2.12	6.55	1.03	2.66	2.07	1.22	3.62	1.64
Sr	625	664	728	622	705	660	545	593	502	426	316	373	303	697	647
Y	35.6	9.40	4.54	19.6	55.1	10.6	11.3	5.39	4.66	3.30	2.95	4.76	5.71	6.60	4.06
Zr	59.2	72.9	13.7	143	226	70.9	74.8	22.5	39.0	10.1	19.9	18.9	8.01	34.6	16.3
Nb	5.20	3.00	1.30	5.56	8.65	3.65	6.37	1.19	2.83	0.64	1.10	1.40	0.80	2.31	1.14
Mo	4.08	0.75	1.53	4.40	11.0	4.78	2.75	3.46	2.07	4.64	7.38	26.1	17.2	1.62	1.61
Cd	0.86	0.27	0.11	1.18	1.05	0.59	0.34	0.08	0.06	0.05	0.03	0.33	0.05	0.37	0.10
Sn	1.93	0.91	0.34	1.13	1.72	1.13	1.82	0.57	0.97	0.73	0.70	0.40	0.27	0.67	0.22
Sb	244	64.1	90.3	268	85.2	280	139	57.0	128	29.9	11.5	12.7	22.1	154	85.7
Cs	9.13	3.46	2.26	12.0	7.83	6.43	15.2	1.83	3.10	0.98	1.50	1.34	1.42	3.50	2.56
Ba	285	321	441	436	440	512	439	269	212	130	104	138	99.0	461	334
Hf	2.42	2.37	2.87	7.77	8.47	4.93	4.46	1.00	2.35	1.57	1.40	1.85	2.05	1.70	1.11
Ta	0.31	0.36	0.08	0.50	0.58	0.39	0.63	0.10	0.34	0.05	0.26	0.09	0.05	0.22	0.08
W	100	53.6	281	493	266	358	265	44.4	140	140	93.0	141	206	89.4	75.8
Tl	3.02	5.49	9.10	6.35	3.71	5.65	7.38	5.28	6.80	6.61	4.09	3.74	2.77	6.94	8.44
Pb	14.0	4.46	2.73	9.27	16.2	6.17	8.36	5.96	5.39	2.57	4.97	9.57	2.01	5.39	3.00
Th	3.61	3.56	1.07	4.73	10.2	4.31	5.23	1.48	4.24	0.84	4.45	1.58	0.60	2.67	1.26
U	86.0	12.0	0.45	72.7	86.6	24.0	22.3	45.0	115	6.22	3.73	0.98	0.61	47.5	22.7
Ash	27.49	22.40	13.93	39.95	38.18	29.12	35.55	17.17	20.78	12.17	14.48	12.47	9.83	22.43	18.83
Rb/Cs	0.48	1.10	0.82	1.33	1.03	1.41	1.84	1.16	2.11	1.05	1.77	1.54	0.86	1.03	0.64
U/Th	23.8	3.37	0.42	15.37	8.49	5.57	4.26	30.4	27.1	7.40	0.84	0.62	1.02	17.79	18.02
Nb/Ta	16.8	8.33	16.3	11.1	14.9	9.36	10.1	11.9	8.32	12.8	4.23	15.6	16.0	10.5	14.3

WL-4 to WL-13 were collected from section a from the top downwards with an interval of 0.4–0.6 m; WL-14 to WL-26 were collected from section b from the top downwards with an interval of 0.5–0.6 m; WL-29 to WL-34 were collected from section c from the top downwards with an interval of 1.4 m. [a]GM and M_1 represent the geometric and arithmetic means of 42 lignite samples from WGD, respectively; [b]Average composition of upper continental crust (Taylor and McLennan, 1985); [c]Average composition of the USA coals (Finkelman, 1993); [d]Average composition of world wide coals (Valkovic, 1983); [e]Average composition of the Chinese coals (Ren et al., 1999; [f]data from Zhao et al., 2002); [g]M_2 stands for average values of two sandstone samples (WL-40 and WL-41); [h]M_3 presents the average values of three Ge-barren lignite samples (HQ-2, HQ-6, and HQ-7) from Hongqi Coal Mine.

	WL-16	WL-17	WL-18	WL-19	WL-20	WL-21	WL-22	WL-23	WL-24	WL-25	WL-26	WL-27	WL-28	WL-29	WL-30
Be	73.9	61.7	68.9	36.9	20.3	14.7	16.3	9.88	31.6	20.6	21.7	133	75.0	16.7	12.2
TiO_2	1747	834	905	675	853	633	210	280	895	1871	250	2242	2187	188	923
MnO	106	95.0	80.7	65.0	44.1	45.9	34.7	25.9	20.4	43.7	24.5	223	51.9	26.1	34.3
Co	37.9	36.8	53.2	21.74	7.86	3.60	23.8	43.7	32.9	26.7	23.2	14.1	13.3	4.94	2.89
Cu	17.8	14.7	9.51	7.13	7.98	8.23	4.45	7.85	6.52	39.8	7.70	75.1	18.6	5.05	7.04
Zn	335	275	219	70.9	18.4	6.94	11.6	9.24	66.0	37.8	16.6	71.5	179	25.1	7.80
Ga	6.56	8.64	4.34	1.57	1.88	3.62	25.5	11.9	8.74	12.1	1.52	12.4	5.50	1.60	2.23
Ge	41.0	23.3	88.4	285	180	303	513	832	446	325	872	133	78.5	329	517
Rb	13.8	2.51	4.01	2.62	3.01	2.46	1.06	1.16	8.03	47.8	2.65	7.14	10.7	0.84	6.57
Sr	606	548	446	302	235	144	80.3	73.9	67.2	73.6	110	871	662	504	217
Y	7.99	4.17	5.57	4.18	2.93	3.13	1.83	2.01	7.52	9.25	8.17	115	23.8	2.41	2.43
Zr	35.3	13.4	35.4	18.1	26.6	27.0	9.69	12.8	31.4	59.7	14.9	104	47.2	9.52	19.4
Nb	2.88	1.23	2.72	0.84	1.80	1.23	0.63	0.60	1.51	4.24	0.54	4.84	3.57	0.59	0.86
Mo	1.65	1.70	2.01	16.8	26.7	8.46	5.58	15.9	3.91	2.85	2.26	3.31	2.20	2.47	11.7
Cd	0.14	0.09	0.15	0.12	0.06	0.03	0.07	0.26	0.29	0.15	0.05	1.61	1.67	0.07	0.02
Sn	1.03	0.42	1.00	0.37	0.45	0.40	0.17	0.19	0.36	1.55	0.56	1.15	0.98	0.25	0.47
Sb	89.2	80.0	89.7	87.7	6.70	5.42	11.5	13.8	7.26	1.81	16.4	228	30.5	180	41.1
Cs	7.71	2.08	3.72	1.72	1.79	1.91	3.49	6.02	8.60	38.9	9.47	9.23	10.8	1.16	3.30
Ba	413	293	242	114	771	52.3	26.3	41.8	76.5	110	83.8	508	228	93.1	61.5
Hf	2.00	1.24	1.70	2.11	1.63	1.48	1.52	2.87	2.03	2.77	3.01	4.13	1.85	0.52	1.06
Ta	0.26	0.09	0.28	0.08	0.13	0.11	0.04	0.04	0.14	0.34	0.03	0.38	0.32	0.04	0.13
W	116	97.2	68.7	173	89.1	81.6	146	269	136	103	266	129	67.2	31.0	61.1
Tl	11.6	11.6	13.5	17.6	13.8	9.61	31.7	30.6	0.40	0.99	0.17	3.75	4.50	6.03	8.57
Pb	6.46	8.01	8.20	3.67	6.41	4.04	0.94	1.87	3.02	18.9	4.80	32.8	8.65	2.14	18.6
Th	3.38	3.07	3.86	1.55	2.21	2.65	0.47	0.82	2.00	7.76	1.56	5.54	3.70	0.51	1.59
U	14.8	9.33	29.3	3.74	3.73	5.57	20.1	8.57	1.77	2.37	0.82	68.7	148	81.8	0.69
Ash	23.30	15.64	21.13	14.23	13.92	12.33	9.56	7.16	14.24	29.16	11.30	29.83	29.05	10.87	13.13
Rb/Cs	1.79	1.21	1.08	1.52	1.68	1.29	0.30	0.19	0.93	1.23	0.28	0.77	0.99	0.72	1.99
U/Th	4.38	3.04	7.59	2.41	1.69	2.10	42.8	10.5	0.89	0.31	0.53	12.4	40.0	160	0.43
Nb/Ta	11.1	13.7	9.71	10.5	13.8	11.2	15.8	15.0	10.8	12.5	18.0	12.7	11.2	14.8	6.62

(*continued on next page*)

Table 1 (*continued*)

	WL-31	WL-32	WL-33	WL-34	WL-35	WL-36	WL-37	WL-38	WL-39	WL-42	WL-43	WL-44	GM[a]	M_1[a]	Min	Max	EF
Be	10.1	20.2	49.9	34.7	18.6	74.5	23.1	44.9	54.3	6.26	5.64	48.0	33.1	43.8	5.64	133	60
TiO_2	532	522	646	167	1061	2618	607	950	2586	994	1752	1799	917	1218	167	3394	1.0
MnO	21.1	17.9	18.9	23.1	58.0	126	28.9	51.8	112	40.7	46.0	103	64.3	82.6	17.9	223	0.4
Co	2.22	1.87	12.4	2.97	15.7	16.1	3.26	6.57	13.0	2.72	4.84	12.0	10.8	15.7	1.87	53.2	6.4
Cu	5.45	7.85	6.94	3.54	13.9	43.4	5.43	10.3	20.3	20.7	25.1	17.0	12.0	15.4	3.54	75.1	2.5
Zn	9.91	9.40	60.1	13.8	109	112	11.8	30.3	216	6.26	10.4	114	48.7	100	4.64	424	5.8
Ga	1.16	1.95	1.96	0.73	6.65	3.65	2.29	3.02	14.2	1.94	2.82	1.80	3.65	5.47	0.48	25.5	1.3
Ge	432	164	254	339	1399	97.3	193	91.4	76.5	256	923	110	168	300	23.3	1424	770
Rb	3.24	2.69	3.99	1.37	22.3	5.96	3.45	11.4	3.89	7.38	17.8	3.34	4.28	6.98	0.84	47.8	0.3
Sr	180	54.8	49.7	56.0	140	706	357	452	584	220	286	605	307	406	49.7	871	4.8
Y	1.90	2.16	4.99	2.09	11.8	23.7	2.88	6.50	15.1	10.8	8.56	16.5	6.68	11.7	1.83	115	2.2
Zr	16.6	13.4	17.8	5.83	41.1	62.2	43.5	33.3	82.5	16.3	25.8	102	29.1	41.8	5.83	226	0.9
Nb	0.60	0.98	1.67	0.47	1.92	5.33	1.05	1.61	4.70	2.18	2.65	3.80	1.77	2.39	0.47	8.65	0.4
Mo	2.58	0.37	0.42	0.85	3.08	1.37	4.46	1.65	3.41	9.35	32.1	2.07	3.58	6.25	0.37	32.1	17
Cd	0.01	0.05	0.06	0.04	0.08	0.49	0.04	0.17	1.12	0.04	0.07	0.18	0.14	0.30	0.01	1.67	13
Sn	0.26	0.28	0.41	0.44	0.63	1.58	0.25	0.68	1.14	0.68	1.08	0.63	0.60	0.74	0.17	1.93	0.6
Sb	62.5	5.17	2.31	11.0	11.2	348	33.8	30.6	79.8	4.91	9.28	84.2	36.5	77.2	1.81	348	1585
Cs	2.12	1.99	5.03	4.52	24.6	4.83	3.32	5.64	4.19	5.27	11.9	4.22	4.23	6.19	0.98	38.9	6.9
Ba	58.2	49.5	107	69.2	223	615	115	263	432	96.2	80.5	282	175	241	26.3	771	1.8
Hf	1.24	0.75	1.11	1.04	4.63	5.25	2.43	2.13	3.08	1.30	2.24	2.95	2.08	2.49	0.52	8.47	1.8
Ta	0.06	0.07	0.11	0.03	0.15	0.49	0.09	0.16	0.47	0.1	0.19	0.38	0.15	0.21	0.03	0.63	0.4
W	87.7	43.3	59.3	95.9	367	373	148	131	80.3	91.3	155	45.5	120	149	31.0	493	306
Tl	5.46	2.76	0.14	0.74	0.48	7.73	3.59	6.45	3.54	1.44	1.20	4.67	4.14	6.86	0.14	31.7	38
Pb	1.89	5.34	7.10	7.79	10.5	29.1	2.71	5.58	11.1	8.45	11.8	3.62	5.97	7.94	0.94	32.8	1.6
Th	1.00	1.15	1.51	0.39	4.47	6.22	2.07	2.00	5.28	3.47	5.55	3.16	2.30	3.02	0.39	10.2	1.2
U	0.58	0.42	0.59	0.65	1.46	19.1	0.74	9.63	66.1	1.00	0.96	40.1	7.11	25.87	0.42	148	38
Ash	10.95	6.86	12.65	8.43	23.21	23.58	14.08	20.46	30.33	13.41	15.79	25.88	17.15	18.93	6.86	39.95	
Rb/Cs	1.53	1.35	0.79	0.30	0.91	1.23	1.04	2.02	0.93	1.40	1.50	0.79	1.01	1.14	0.19	2.11	
U/Th	0.58	0.37	0.39	1.67	0.33	3.07	0.36	4.82	12.5	0.29	0.17	12.7	3.09	11.7	0.17	160	
Nb/Ta	10.0	14.0	15.2	15.7	12.8	10.9	11.7	10.1	10.0	21.8	13.9	10.0	12.0	12.5	4.23	21.8	

	UCC[b]	USA[c]	WWC[d]	CC[e]	M_1/UCC	M_1/USA	M_1/WWC	M_1/CC	WL-40	WL-41	M_2[g]	HQ-2	HQ-6	HQ-7	M_3[h]	M_1/M_2	M_1/M_3
Be	3	2.2	3	2[f]	14.6	19.9	14.6	21.9	0.89	1.31	1.10	1.17	0.72	1.04	0.98	39.8	44.9
TiO_2	5000	1334	834	2812	0.24	0.91	1.46	0.43	1199	2296	1748	769	590	1193	851	0.70	1.43
MnO	775	129	64.6	350	0.11	0.64	1.28	0.24	410	399	405	734	102	150	329	0.20	0.25
Co	10	6.1	5	6.72	1.57	2.58	3.15	2.34	1.93	3.02	2.48	24.6	2.7	2.56	9.95	6.36	1.58
Cu	25	16	15	28.2	0.61	0.96	1.02	0.55	4.73	6.97	5.85	66.6	4.02	8.56	26.4	2.63	0.58
Zn	71	53	50	43.2	1.41	1.89	2.00	2.32	8.2	25.6	16.9	187	12.9	17.4	72.4	5.92	1.38
Ga	17	5.7	7	81.1	0.32	0.96	0.78	0.07	7.64	8.52	8.08	3.26	2.61	3.85	3.24	0.68	1.69
Ge	1.6	5.7	5		187	53	59.9		12.3	2.96	7.63	0.35	0.85	1.03	0.74	39.3	403
Rb	112	21	100	20.7	0.06	0.33	0.07	0.34	72.9	88.9	80.9	16.3	8.97	13.0	12.8	0.09	0.55
Sr	350	130	500	176	1.16	3.12	0.81	2.30	74.3	73.0	73.7	117	77.7	103	99.2	5.51	4.09
Y	22	8.5	10	2[f]	0.53	1.38	1.17	1.46	2.95	8.95	5.95	8.26	4.49	7.83	6.86	1.96	1.70
Zr	190	27		247	0.22	1.55		0.17	71.7	98.0	84.9	36.3	49.2	91.1	58.9	0.49	0.71
Nb	25	2.9		14[f]	0.10	0.82		0.17	2.01	5.21	3.61	7.86	5.82	7.29	6.99	0.66	0.34
Mo	1.5	3.3	5	18.2	4.17	1.89	1.25	0.34	0.59	0.53	0.56	1.12	0.68	0.91	0.90	11.2	6.92
Cd	0.098	0.47		0.46	3.06	0.64		0.65	0.04	0.01	0.03	0.24	0.02	0.04	0.10	12.0	3.00
Sn	5.5	1.3		2[f]	0.13	0.57		0.37	0.78	2.40	1.59	0.54	0.54	0.97	0.68	0.46	1.08
Sb	0.2	1.2	3	2.56	386	64.4	25.7	30.2	2.84	1.41	2.13	0.29	0.32	0.38	0.33	36.3	234
Cs	3.7	1.1		2.21	1.67	5.6		2.80	8.00	15.1	8.0	1.96	0.98	1.54	1.49	0.78	4.15
Ba	550	170	500	169	0.44	1.42	0.48	1.43	412	315	364	94.9	33.9	150	92.9	0.66	2.59
Hf	5.8	0.73		3.26	0.43	3.40		0.76	2.27	3.06	2.67	1.15	1.33	2.52	1.67	0.93	1.49
Ta	2.2	0.22		3.91	0.09	0.95		0.05	0.18	0.48	0.33	0.18	0.41	1.01	0.53	0.63	0.39
W	2	1		2.35	74.5	149		63.4	12.7	5.18	8.94	1.89	1.08	1.07	1.35	16.7	111
Tl	0.75	1.2		0.4[f]	9.14	5.7		17.1	0.53	0.56	0.55	0.22	0.40	0.13	0.25	12.6	27.4
Pb	20	11	25	24.8	0.40	0.72	0.32	0.32	8.53	9.88	9.21	4.54	3.75	2.52	3.60	0.86	2.20
Th	10.7	3.2		6.9	0.28	0.94		0.44	2.29	4.43	3.36	1.81	1.34	2.55	1.90	0.90	1.59
U	2.8	2.1	1	7.52	9.24	12.3	25.9	3.44	0.58	1.64	1.11	0.73	0.43	0.48	0.55	23.3	47.3
Ash		13.1										11.69	9.01	14.31	11.67		
Rb/Cs	30.3	19.09	30.3						9.11	5.89	7.50	8.32	9.15	8.44	8.64		
U/Th	0.26	0.66	0.26						0.25	0.37	0.31	0.40	0.32	0.19	0.30		
Nb/Ta	11.4	13.2	11.4						11.2	10.9	11.0	43.7	14.2	7.22	21.7		

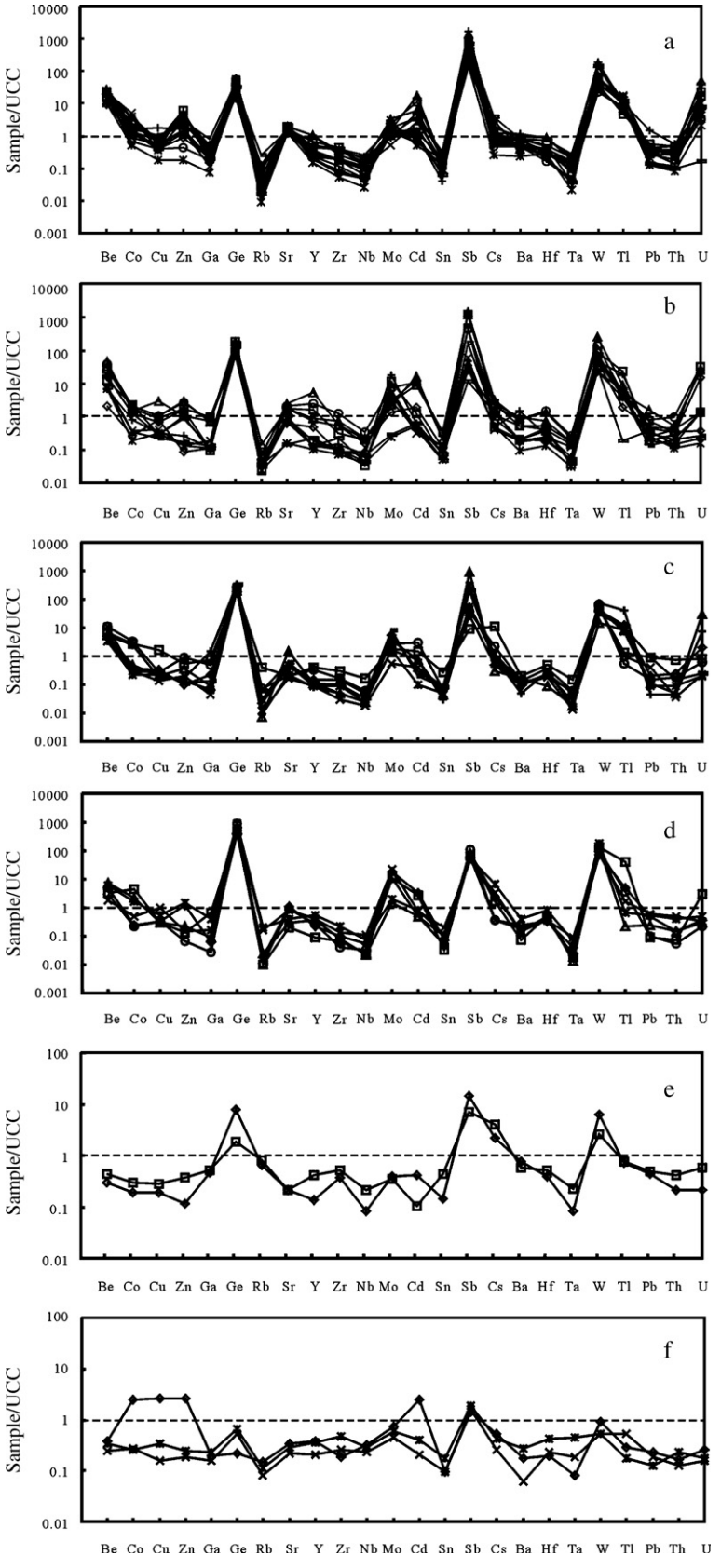
a
b
c
d
e
f
Sample/UCC
Be Co Cu Zn Ga Ge Rb Sr Y Zr Nb Mo Cd Sn Sb Cs Ba Hf Ta W Tl Pb Th U

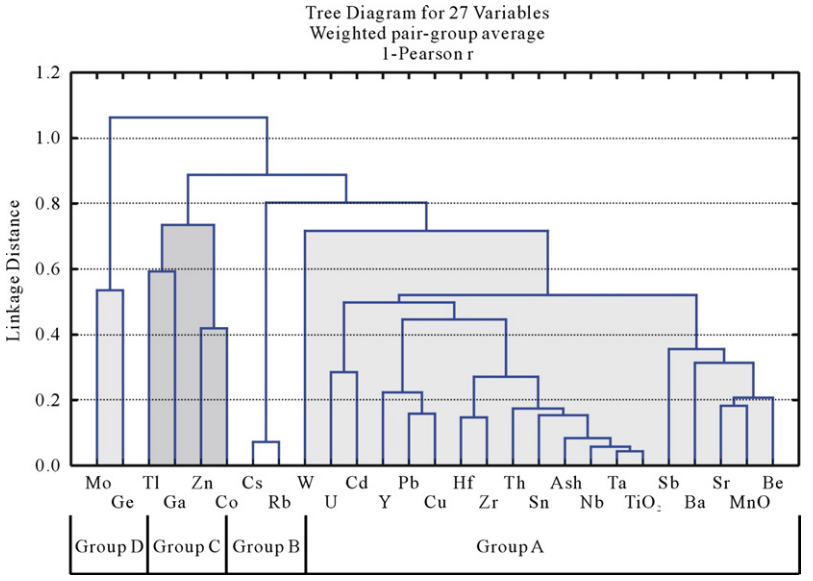

Fig. 5. Dendrogram produced by cluster analysis of analytical data of 42 lignite samples from WGD ($n=42$, $p<0.05$).

times). The average concentrations of Ta, Nb, MnO, Sn, Zr, TiO_2, Th, Ga, Pb, Hf, Ba, Y, and Cu are lower than those of upper continental crust (from 0.09 to 0.61 times).

The enrichment factor (EF) of trace elements in the lignite from WGD were calculated using TiO_2 as reference element and the following formula:

$$EF = \frac{\text{element}_i/\text{TiO}_{2(\text{coal})}}{\text{element}_i/\text{TiO}_{2(\text{UCC})}} \quad (1)$$

where $element_i$ and TiO_2 represent the concentration average of element i and TiO_2 in lignite from WGD and upper continental crust (Taylor and McLennan, 1985), respectively. The EF values of Rb, Nb, Ta, MnO, Sn, and Zr range from 0.3 to 0.9, while EF values for Cu, Co, Zn, Ga, Sr, Y, Cs, Ba, Hf, Pb, and Th vary from 1.2 to 6.9. Elements with EF values more than 10 include Sb (1585), Ge (770), W (306), Be (60), Tl (38), U (38), Mo (17), and Cd (13) (Table 1).

Compared with the average concentrations of elements in the USA coals (Finkelman, 1993), U, Be, Ge, Sb, and W are 12.3–64.4 times higher. The average concentration of Y, Ba, Zr, Zn, Mo, Co, Hf, Sr, and Tl are slightly (1.38–5.7 times) higher. The average contents of TiO_2, MnO, Ga, Cu, Rb. Nb, Cd, Sn, Ta, Pb, and Th are lower than those of USA coals. The distinct enrichment of Be, Sb, U, and Ge in the lignite from WGD also can be seen when compared to the average concentrations of these elements with those of worldwide coals (from Valkovic, 1983). The lignites of WGD are obviously enriched in Sb, W, Be, and Tl, compared to the average composition of elements in the Chinese coals (Ren et al., 1999; Zhao et al., 2002).

It is noted that the two samples of sandstone collected from the overlying strata of the No.6-1 coal seam are distinctly enriched in Ge, Sb, Cs, and W, and slightly depleted in most of the remaining elements in comparison with those of upper continental crust (Fig. 4e). One lignite sample from Hongqi Coal Mine shows slight enrichment of Co, Cu, Zn, Cd, and Sb, and the other two lignite samples from Hongqi Coal Mine only slightly enriched in Sb, while most elements in them are depleted, compared with those of upper continental crust (Fig. 4f). The frequency distribution curves of most elements, as well as ash yields, are in accordance with the log normal distribution, only the frequency distribution curve of Sr consists of three peaks (Appendix I).

4.2. Geochemical associations and affinity of the elements in lignite from WGD

The cluster analysis classified elements into four associations or groups (Fig. 5).

Fig. 4. Upper Continental Crust (UCC)-normalized trace element composition of different samples from WGD and Hongqi Coal Mine. a. lignite samples with 23.3–97.3 ppm Ge; b. lignite samples with 110–288 ppm Ge; c. lignite samples with 303–517 ppm Ge; d. lignite samples with 672–1424 ppm Ge; e. sandstone samples from WGD; f. lignite samples from Hongqi Coal Mine.

Table 2
Correlation matrix of trace elements and Ash yields of the lignites from the Wulantuga Germanium Deposit (N=42, p<0.05)

	Be	TiO_2	MnO	Co	Cu	Zn	Ga	Ge	Rb	Sr	Y	Zr	Nb	Mo
Be	1.00	0.64	0.80	0.39	0.61	0.65	0.32	−0.54	0.03	0.78	0.69	0.65	0.66	−0.38
TiO_2	0.64	1.00	0.67	0.12	0.69	0.43	0.37	−0.32	0.50	0.59	0.53	0.82	0.95	−0.09
MnO	0.80	0.67	1.00	0.23	0.60	0.57	0.28	−0.45	0.09	0.82	0.57	0.63	0.66	−0.21
Co	0.39	0.12	0.23	1.00	0.10	0.58	0.42	−0.12	0.13	0.14	0.03	0.10	0.15	−0.21
Cu	0.61	0.69	0.60	0.10	1.00	0.20	0.35	−0.18	0.45	0.50	0.83	0.55	0.69	−0.08
Zn	0.65	0.43	0.57	0.58	0.20	1.00	0.16	−0.40	0.06	0.62	0.10	0.29	0.36	−0.31
Ga	0.32	0.37	0.28	0.42	0.35	0.16	1.00	−0.04	0.26	0.09	0.37	0.39	0.44	−0.12
Ge	−0.54	−0.32	−0.45	−0.12	−0.18	−0.40	−0.04	1.00	0.10	−0.55	−0.14	−0.24	−0.31	0.46
Rb	0.03	0.50	0.09	0.13	0.45	0.06	0.26	0.10	1.00	−0.07	0.10	0.29	0.45	−0.04
Sr	0.78	0.59	0.82	0.14	0.50	0.62	0.09	−0.55	−0.07	1.00	0.50	0.51	0.57	−0.24
Y	0.69	0.53	0.57	0.03	0.83	0.10	0.37	−0.14	0.10	0.50	1.00	0.62	0.61	−0.08
Zr	0.65	0.82	0.63	0.10	0.55	0.29	0.39	−0.24	0.29	0.51	0.62	1.00	0.89	−0.10
Nb	0.66	0.95	0.66	0.15	0.69	0.36	0.44	−0.31	0.45	0.57	0.61	0.89	1.00	−0.11
Mo	−0.38	−0.09	−0.21	−0.21	−0.08	−0.31	−0.12	0.46	−0.04	−0.24	−0.08	−0.10	−0.11	1.00
Cd	0.72	0.69	0.55	0.10	0.63	0.32	0.46	−0.24	0.12	0.57	0.75	0.66	0.69	−0.11
Sn	0.54	0.85	0.58	0.14	0.66	0.27	0.38	−0.29	0.55	0.48	0.50	0.66	0.89	−0.12
Sb	0.66	0.56	0.72	0.17	0.55	0.41	0.21	−0.37	0.02	0.70	0.44	0.44	0.55	−0.28
Cs	0.04	0.40	0.03	0.21	0.45	0.02	0.35	0.25	0.93	−0.15	0.19	0.28	0.40	−0.10
Ba	0.67	0.63	0.69	0.19	0.50	0.54	0.13	−0.45	0.08	0.71	0.40	0.50	0.60	−0.07
Hf	0.53	0.75	0.60	0.17	0.52	0.22	0.38	0.03	0.35	0.40	0.50	0.85	0.78	−0.02
Ta	0.61	0.96	0.68	0.14	0.64	0.38	0.36	−0.38	0.45	0.59	0.49	0.82	0.94	−0.19
W	0.22	0.39	0.36	0.17	0.25	0.07	0.23	0.30	0.26	0.14	0.14	0.37	0.35	0.06
Tl	−0.08	−0.22	−0.05	0.45	−0.20	0.03	0.41	−0.03	−0.25	−0.08	−0.19	−0.19	−0.21	0.17
Pb	0.47	0.56	0.39	−0.01	0.84	0.05	0.25	−0.08	0.36	0.31	0.72	0.45	0.59	0.01
Th	0.47	0.84	0.53	0.15	0.70	0.26	0.36	−0.18	0.59	0.38	0.53	0.78	0.87	0.00
U	0.54	0.47	0.53	0.08	0.30	0.33	0.32	−0.34	0.00	0.58	0.45	0.49	0.53	−0.24
Ash	0.72	0.93	0.74	0.23	0.64	0.53	0.41	−0.35	0.53	0.65	0.54	0.84	0.91	−0.24

The first association (Group D) includes Ge and Mo. They are negatively correlated with ash yield (r_{Ge-Ash}=−0.35, r_{Mo-Ash}=−0.24, Table 2). Germanium has a higher correlation coefficient with Mo (r=0.46, Table 2) than other elements. Low ash coals are rich in Ge and Mo (Appendix II). No Ge- or Mo-bearing minerals were identified by SEM-EDX. These facts suggest that Ge and Mo have mainly organic affinity. Mo also shows an organic affinity in some Greek lignites (Foscolos et al., 1989), and some bituminous and anthracite coals from western Guizhou, China (Dai et al., 2005).

The second association (Group C) is Tl–Ga–Zn–Co. The correlation coefficients between these elements and ash yields range from −0.22 to 0.53 (Table 2). Low- and moderate-ash coals have higher content of these elements than high-ash coals (Appendix II). The elements in this association, possibly including As, mainly associated with mineral matter (such as sphalerite, etc., Fig. 6), but organic affinity was not excluded.

The third association is Rb–Cs (Group B). Similar correlation coefficients with ash yields (r_{Rb-Ash}=0.53, r_{Rb-Ash}=0.48, Table 2) and high correlation between them (r_{Rb-Cs}=0.93, Table 2) may indicate similar modes of occurrence of Rb and Cs in the lignite of WGD. Rubidium commonly shows positive correlation with illite, Al_2O_3 and K_2O (Dypvik and Harris, 2001). Average claystones and siltstones are normally enriched in Rb (Taylor, 1965; Fralick and Kronberg, 1997). It is generally thought that these two elements have mainly aluminosilicate affinity (associated with K minerals; Goodarzi, 1988, and references therein).

The last association (Group A) includes W–U–Cd–Y–Pb–Cu–Hf–Zr–Th–Sn–Nb–Ta–Ti–Sb–Ba–Sr–Mn–Be. Most elements in this association have high correlation coefficients (from 0.54 to 0.91, Table 2) with ash yield, with an exception of W (r_{W-Ash}=0.37) and Pb (r_{Pb-Ash}=0.48). High-ash coals are enriched in these elements (Appendix II). The elements of Group A (including Bi) possibly are mainly associated with mineral matter (such as anatase, manganite, zircon, barite etc, Figs. 7 and 8) and have mainly aluminosilicate affinity.

Silver-bearing particles or native Ag were usually identified by SEM-EDX in the lignites from WGD and Hongqi Coal Mine, these minerals generally are irregular laminar grains, with a width up to 10 μm (Fig. 9). The existence of these Ag-bearing particles indicates that the lignite of Shengli Coalfield may contain considerable Ag mineralization.

Cd	Sn	Sb	Cs	Ba	Hf	Ta	W	Tl	Pb	Th	U	Ash
0.72	0.54	0.66	0.04	0.67	0.53	0.61	0.22	−0.08	0.47	0.47	0.54	0.72
0.69	0.85	0.56	0.40	0.63	0.75	0.96	0.39	−0.22	0.56	0.84	0.47	0.93
0.55	0.58	0.72	0.03	0.69	0.60	0.68	0.36	−0.05	0.39	0.53	0.53	0.74
0.10	0.14	0.17	0.21	0.19	0.17	0.14	0.17	0.45	−0.01	0.15	0.08	0.23
0.63	0.66	0.55	0.45	0.50	0.52	0.64	0.25	−0.20	0.84	0.70	0.30	0.64
0.32	0.27	0.41	0.02	0.54	0.22	0.38	0.07	0.03	0.05	0.26	0.33	0.53
0.46	0.38	0.21	0.35	0.13	0.38	0.36	0.23	0.41	0.25	0.36	0.32	0.41
−0.24	−0.29	−0.37	0.25	−0.45	0.03	−0.38	0.30	−0.03	−0.08	−0.18	−0.34	−0.35
0.12	0.55	0.02	0.93	0.08	0.35	0.45	0.26	−0.25	0.36	0.59	0.00	0.53
0.57	0.48	0.70	−0.15	0.71	0.40	0.59	0.14	−0.08	0.31	0.38	0.58	0.65
0.75	0.50	0.44	0.19	0.40	0.50	0.49	0.14	−0.19	0.72	0.53	0.45	0.54
0.66	0.66	0.44	0.28	0.50	0.85	0.82	0.37	−0.19	0.45	0.78	0.49	0.84
0.69	0.89	0.55	0.40	0.60	0.78	0.94	0.35	−0.21	0.59	0.87	0.53	0.91
−0.11	−0.12	−0.28	−0.10	−0.07	−0.02	−0.19	0.06	0.17	0.01	0.00	−0.24	−0.24
1.00	0.54	0.48	0.19	0.45	0.56	0.63	0.23	−0.13	0.52	0.51	0.71	0.71
0.54	1.00	0.54	0.50	0.48	0.61	0.86	0.29	−0.27	0.62	0.83	0.44	0.82
0.48	0.54	1.00	−0.02	0.61	0.52	0.58	0.44	−0.01	0.45	0.34	0.45	0.57
0.19	0.50	−0.02	1.00	0.01	0.37	0.35	0.30	−0.26	0.39	0.55	0.03	0.48
0.45	0.48	0.61	0.01	1.00	0.50	0.60	0.32	0.00	0.38	0.44	0.29	0.62
0.56	0.61	0.52	0.37	0.50	1.00	0.72	0.80	−0.09	0.43	0.70	0.29	0.75
0.63	0.86	0.58	0.35	0.60	0.72	1.00	0.33	−0.18	0.52	0.83	0.50	0.91
0.23	0.29	0.44	0.30	0.32	0.80	0.33	1.00	0.07	0.18	0.31	−0.02	0.37
−0.13	−0.27	−0.01	−0.26	0.00	−0.09	−0.18	0.07	1.00	−0.25	−0.28	−0.06	−0.22
0.52	0.62	0.45	0.39	0.38	0.43	0.52	0.18	−0.25	1.00	0.64	0.21	0.48
0.51	0.83	0.34	0.55	0.44	0.70	0.83	0.31	−0.28	0.64	1.00	0.36	0.79
0.71	0.44	0.45	0.03	0.29	0.29	0.50	−0.02	−0.06	0.21	0.36	1.00	0.57
0.71	0.82	0.57	0.48	0.62	0.75	0.91	0.37	−0.22	0.48	0.79	0.57	1.00

4.3. Trace element profiles of the No.6-1 coal seam from WGD

For their moderate to high correlation coefficients with ash yields, most elements of Group A are usually have a tendency with ash yield in different sections (Appendix III). The elements of Group B and Group C more or less follow the distribution of ash yield. For example, profiles of TiO_2 reveal that there is a general increasing tendency from the bottom to top in section a and section b, a distinct high concentration peak near the bottom of section b, and two high concentration peaks in the upper and lower portions within section c. Uranium is mainly concentrated in the middle and top portions, W tends to be concentrated in the top and lower portions, Be mainly concentrated in the top portion. Thallium mainly concentrated in the middle portion of three sections (Fig. 10).

Molybdenum generally follows the distribution of Ge (Appendix III and Fig. 10), and can be concentrated in different portions of different sections. Profiles of Ge and Mo are distinctly distinguished from those of TiO_2, indicating that organic matter plays an important role in their concentration profile (Rasmussen et al., 1998; Gobeil et al., 1999; Bilali et al., 2002).

4.4. TiO_2-normalized profile of trace elements in lignite of the No.6-1 coal seam

The TiO_2 content of the lignites from WGD ranges from 167 to 3394 ppm, positively correlated with ash yields ($r=0.93$, $n=42$, Table 2), and Ti mainly exists in mineral phase (Fig. 7), indicating detrital materials of terrigenous origin. Titanium-normalized profiles of elements in soils, peats and sediments can be used to distinguish elements derived from a clastic source from others, such as the elements derived from weathering of granodioritice crust (Nesbitt and Markovics, 1997), from atmospheric dust deposition (Weiss et al., 2002), or from hydrothermal alteration (Magenheim and Gieskes, 1992; Sturz et al., 1996).

In this case, the contents of trace elements in the samples collected from three sections were normalized toTiO_2. The average values of corresponding ratios of the overlying sandstone from WGD and lignites from Hongqi Coal Mine were calculated as the reference guideline for comparison. The former may represent the background value of the input of detrital materials, and the latter may reflect the background value of various sources (detrital materials or solution) input during coal

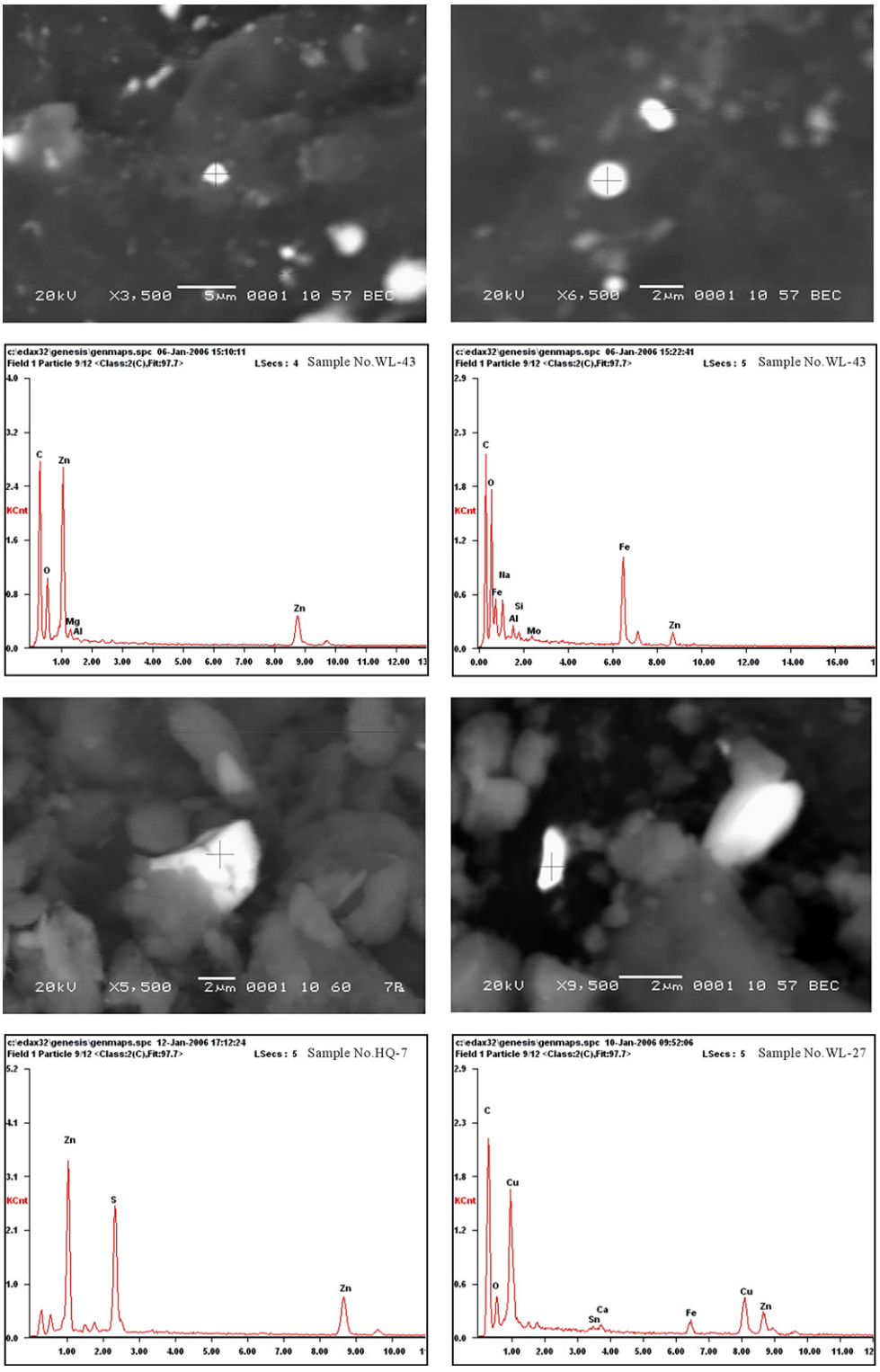

Fig. 6. Selected SEM microphotographs and EDX spectra of micron-sized Zn-bearing minerals.

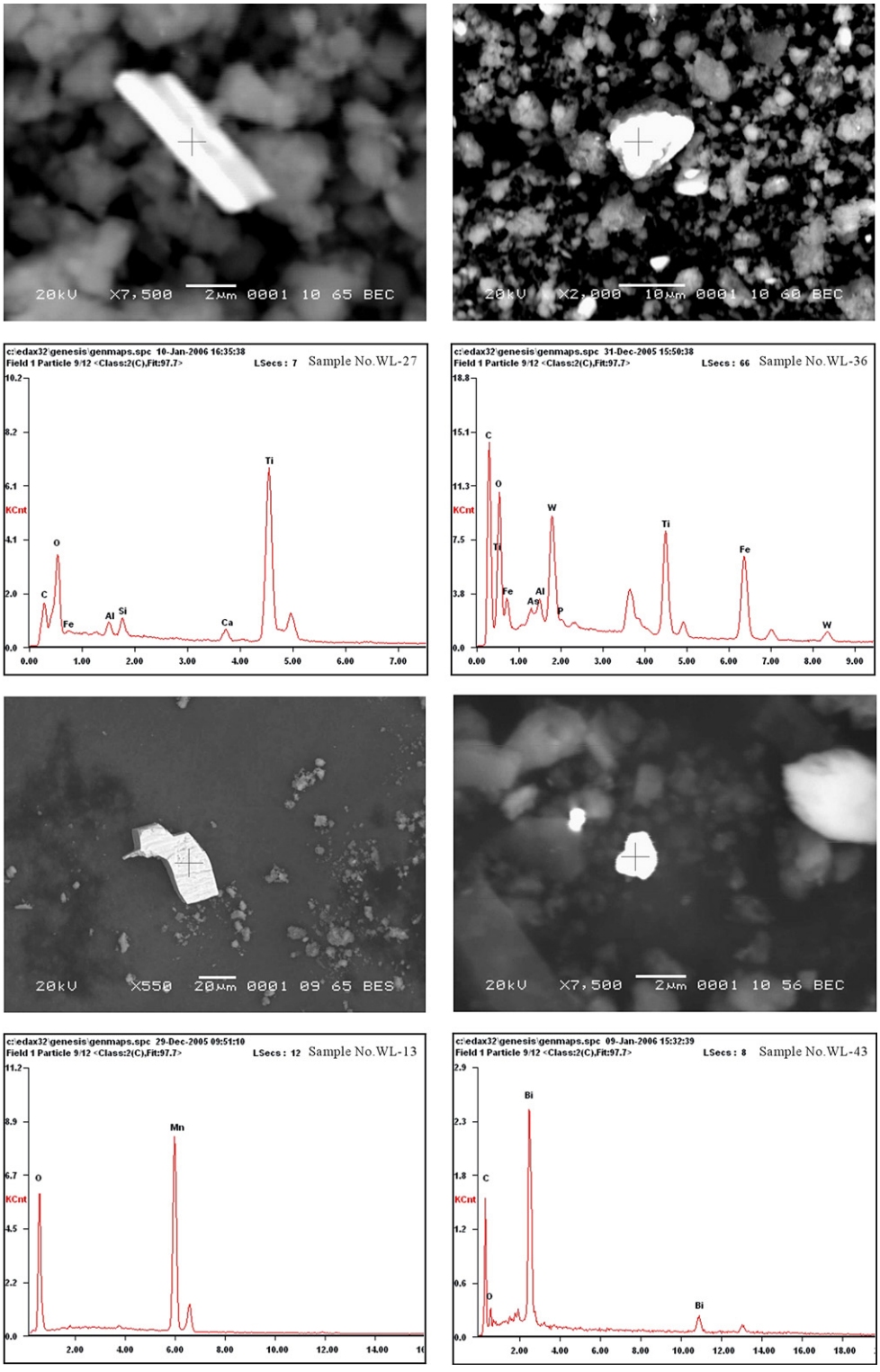

Fig. 7. Selected SEM microphotographs and EDX spectra of micron-sized Ti, W, Mn and Bi-bearing minerals.

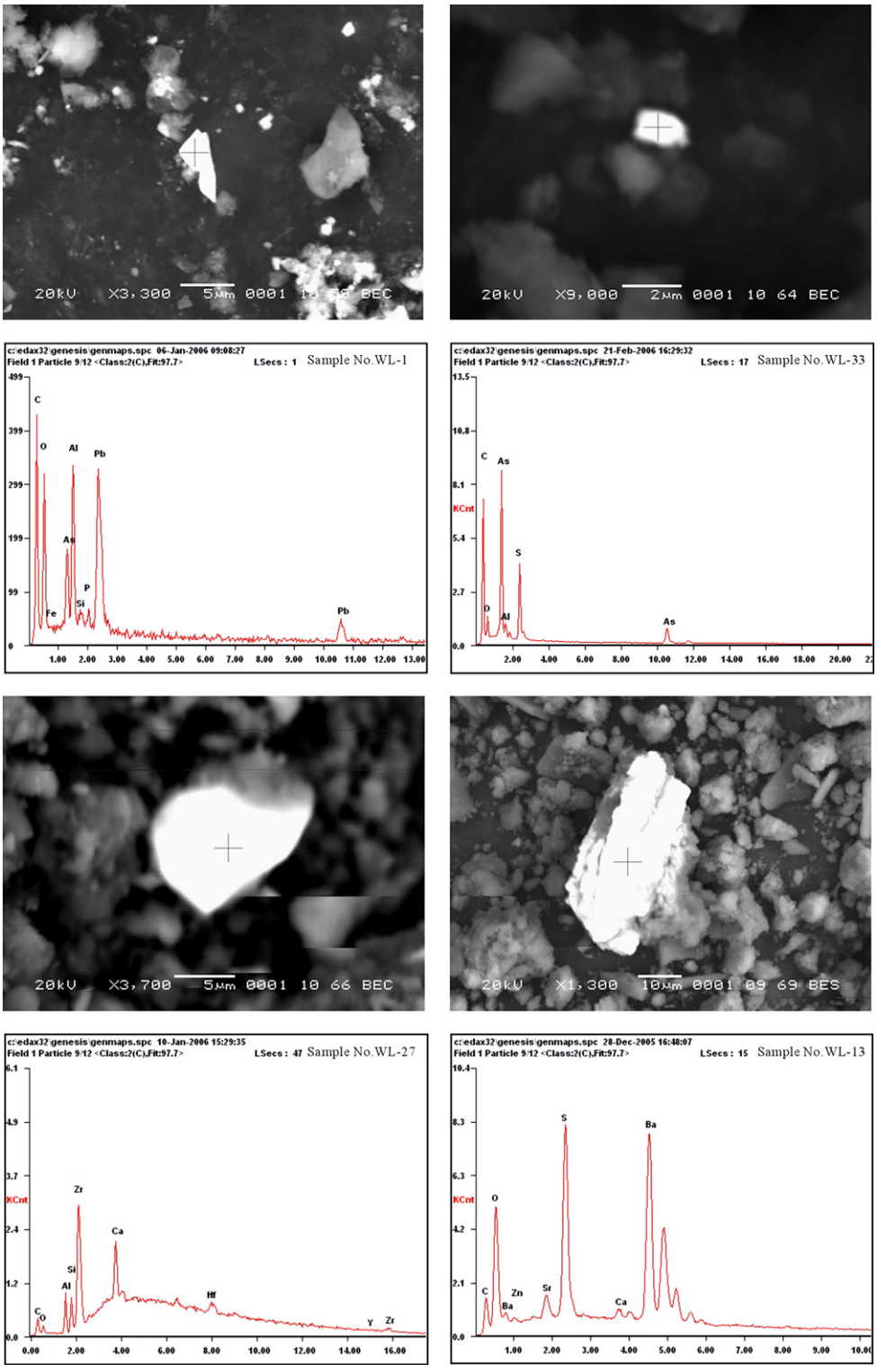

Fig. 8. Selected SEM microphotographs and EDX spectra of micron-sized Pb, As, Zr and Ba-bearing minerals.

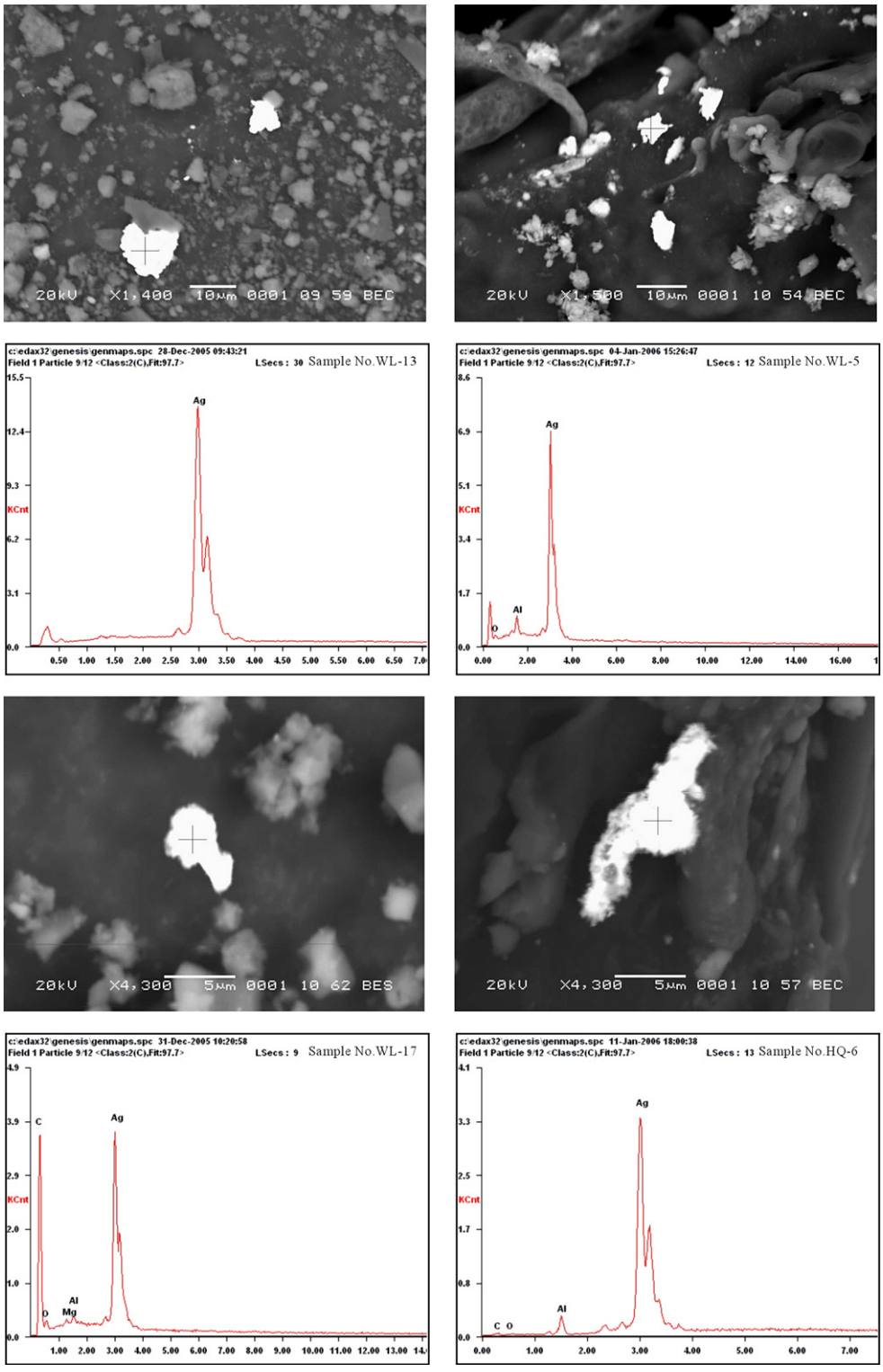

Fig. 9. Selected SEM microphotographs and EDX spectra of micron-sized Ag-bearing minerals.

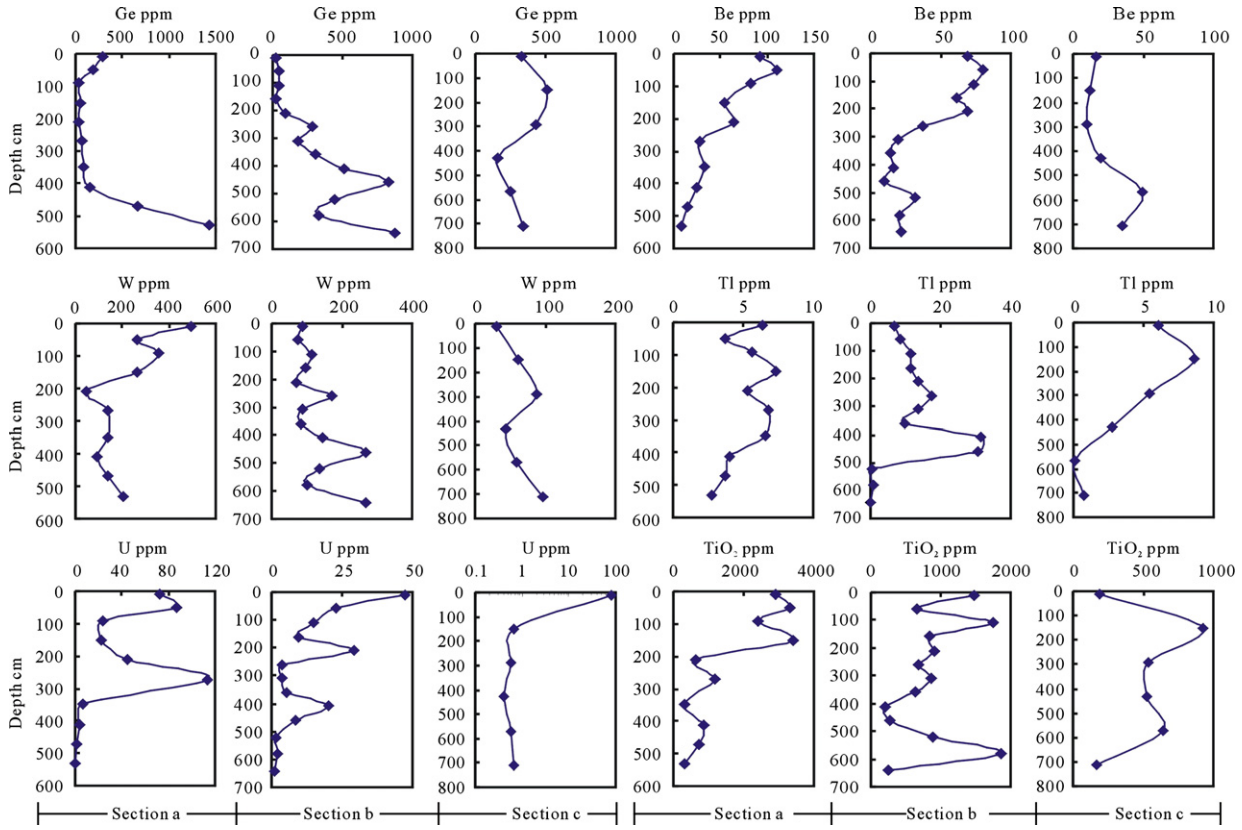

Fig. 10. Elemental concentration profiles of Ge, Be, W, Tl, U, and TiO_2 of lignite in three sections from WGD.

formation and later history without Ge mineralization. All these ratios were simplified as element$_i$/Ti and multiplied by 1000 for convenience of quote and drawing Figs (Appendix IV).

Ratios, including Be/TiO_2, Ge/TiO_2, W/TiO_2, U/TiO_2, Mo/TiO_2, Sb/TiO_2, Tl/TiO_2, and Sr/TiO_2, that from three sections of WGD are generally one or two fold higher than those of sandstone from WGD and lignite from Hongqi Coal Mine (Fig. 11 and Appendix IV). In addition, Be, Ge, W, U, Mo, Sb, Tl, and Sr were enriched in Ge-bearing lignite of WGD compared with those in sandstone of WGD or lignite of Hongqi Coal Mine (Table 1). Thus, it can be seen that besides the input of these elements by detrital materials, much of the contribution may be transported by solution penetrating into coal seam and then concentrated in organic matter by complex physical–chemical sorption or reduction (Bouška, 1981; Valkovic, 1983; Ilger et al., 1987; Foscolos et al., 1989).

The ratio of element/TiO_2 of detrital materials input into coal seam is similar to that of sandstone. The quantity of one element input into lignite of WGD by detrital materials ($Element_i^{DM}$) or by solution ($Element_i^{SO}$) can be estimated by the following formulas:

$$\mathrm{Element_i^{DM}} = \left(\frac{\mathrm{Element_i}}{\mathrm{TiO_2}}\right)_{\mathrm{Sandstone}} \times (\mathrm{TiO_2})_{Lignite} \qquad (2)$$

$$\mathrm{Element_i^{SO}} = \mathrm{Element_i} - \mathrm{Element_i^{DM}} \qquad (3)$$

The average composition of lignite and sandstone from WGD were used, and calculation result show that more than 90% of total contents of Be, Ge, W, U, Mo, Sb, Tl, and Sr were transported by solution.

Ratios of Ba/TiO_2, Co/TiO_2, Cd/TiO_2, and Zn/TiO_2 of the lignite from WGD are generally higher than those of the overlying sandstone from WGD, and close to those of lignite from Hongqi Coal Mine, possibly attributed to the concentration of sulfides, because Ba and Zn mainly occur in barite and sphalerite, as identified by SEM-EDX analysis. Zhuang et al. (2006) found that the lower portion of the No.6-1 coal seam has a higher sulfide content than the upper one. Ratios of MnO/TiO_2, Zr/TiO_2, and Rb/TiO_2 are generally less

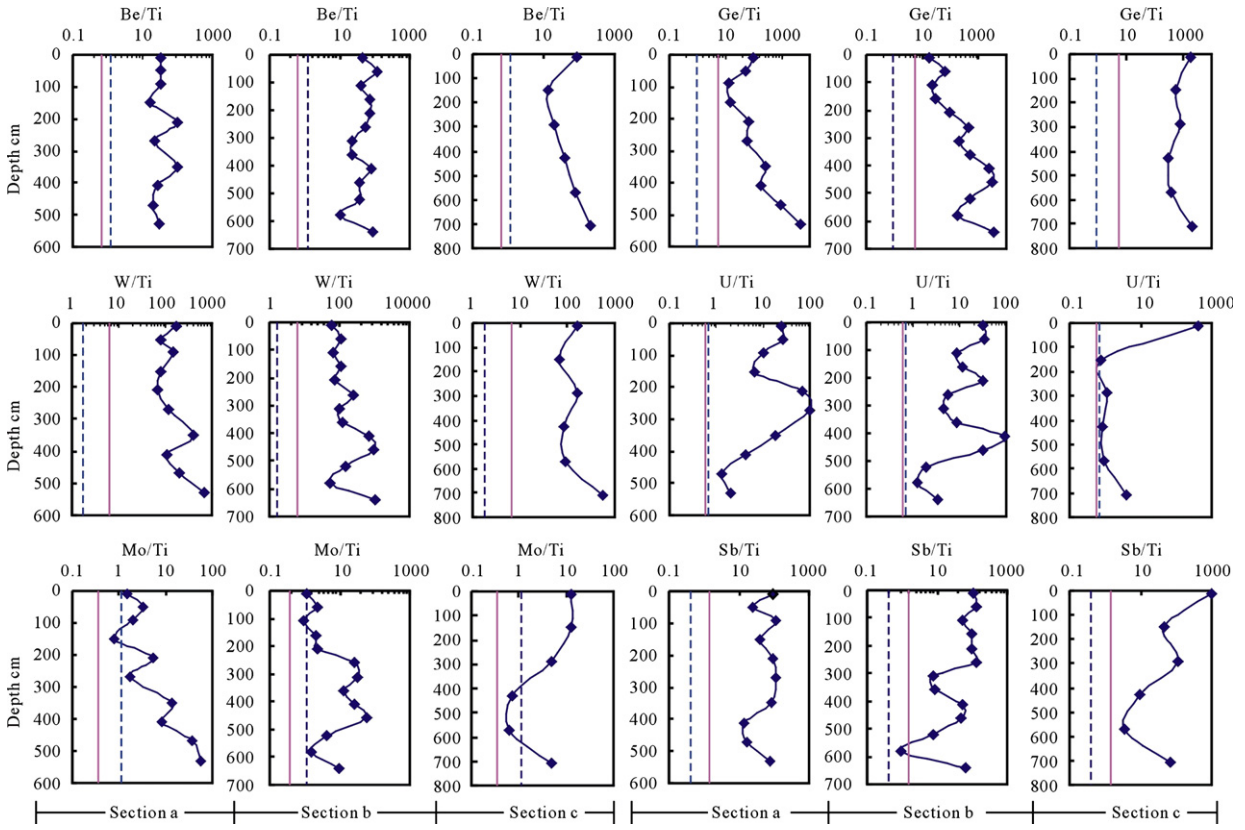

Fig. 11. TiO_2-normalized profiles of Be, Ge, W, U, Mo, and Sb in the lignite in three sections from WGD. Dashed line stands for the corresponding ratios of lignite from Hongqi Coal Mine, Solid line represents those of sandstone from WGD.

than the reference ratios of sandstone from WGD and lignites from the Hongqi Coal Mine, which may be caused by sedimentary sorting during the peat accumulation. Zirconium and Rb are commonly associated with the relatively coarse-grained fraction and with relatively fine-grained fraction of siliciclastic sediments (Dypvik and Harris, 2001). The remaining ratios of element/TiO_2 of the lignite in three sections from WGD fluctuate from top to bottom, but their average values are close to those of the sandstone from WGD or lignite from the Hongqi Coal Mine, indicate these elements mainly originated from detrital materials (Appendix IV).

4.5. Ratios of Rb/Cs, U/Th, and Nb/Ta vs. Ge contents in the lignite from WGD

The Rb/Cs ratio lignites from WGD varies from 0.2 to 2.1, which is similar to that (0.9–2.1) of the Ge-bearing lignite from Spetsugli Germanium Deposit, Russian Far East (Seredin, 2003) and that (0.74–1.8) of Ge-bearing lignite from LGD, Yunnan, China (Qi et al., 2004), but distinctly lower than that (5.9–9.1) of the sandstone from WGD and that (8.3–9.2) of the lignite from Hongqi Coal Mine, as well as the ratios (8.2–14.0) of the low sulfur Amos coal, Western Kentucky coalfield, USA (Hower et al., 2002) and that (19) of the average coal of the USA (Finkelman, 1993). However, lower Rb/Cs ratios are not the unique characteristics of Ge-bearing lignite. For example, high Rb/Cs ratio (2.4–11) can be found in the Ge-bearing lignite from Luzanovka, Russian Far East (Seredin, 2006), and lower ratios also can be found in the lignite from Beypazari lignite, central Anatolia, Turkey (2.0–3.4, with an exception of two anomalous values) (Querol et al., 1997), and the Lower Pliocene fossiliferous Kangal lignites, Sivas, Turkey (0.9–1.3) (Karayigit et al., 2001) (Fig. 12I). The difference of source rocks and changes of input of fine-grained siliciclastic detritus during peat accumulation may contribute to variations of Rb/Cs ratio in different lignites.

The U/Th ratio of lignites from WGD generally varies from 0.17 to 42.8, and the maximum ratio is up to 160. Nearly 70% of all 42 samples have U/Th ratios higher than 1, while the remaining samples have U/Th ratios less than 1. Similar ratios (generally higher than 1)

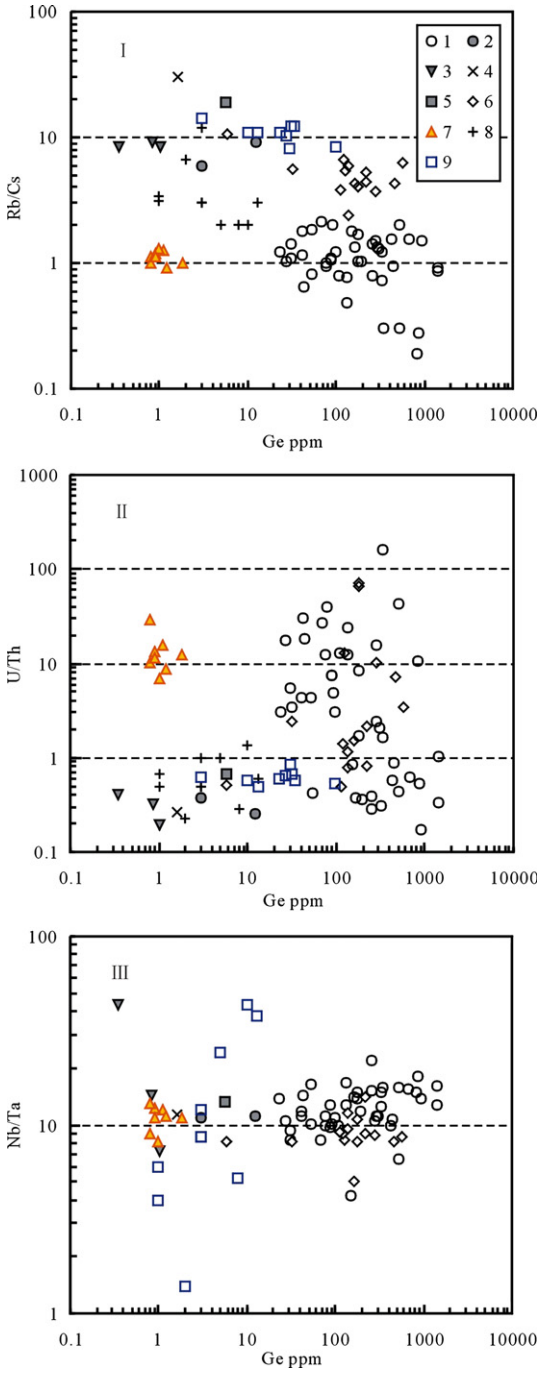

Fig. 12. Scatter diagram of Ge vs. ratios of Rb/Cs, U/Th, and Nb/Ta of lignite and sandstone from WGD, as well as other lignite from different locations (calculated according to the elemental concentration data published in the references). 1 Ge-bearing lignite from WGD; 2 sandstone from WGD; 3 lignite from Hongqi Coal Mine; 4 Upper Continental Crust (Taylor and McLennan, 1985); 5 average of the USA coals (Finkelman, 1993); 6 Ge-bearing lignite from Luzanovka Germanium Deposit, Russian Far East (Seredin, 2006); 7 low sulfur Amos coal, Western Kentucky coalfield, USA (Hower et al., 2002); 8. Lower Pliocene fossiliferous Kangal lignites, Sivas,Turkey (Karayigit et al., 2001); 9 Beypazari lignite, central Anatolia, Turkey (Querol et al., 1997).

also can be found in Ge-bearing lignite from LGD and Luzanovka of GDRFE (Qi et al., 2004; Seredin, 2006). It is found that most coals, as well as sandstone from WGD and upper continental crust (Taylor and McLennan, 1985), have U/Th ratios less than 1: for example, lignite from Hongqi Coal Mine; Amos (Hower et al., 2002); Anatolia (Querol et al., 1997); the average of the USA coals (Finkelman, 1993); thermally metamorphosed bituminous coal (Finkelman et al., 1998); and the Fire Clay coal bed, Eastern Kentucky (Hower et al., 1999). Lignites with relative higher U contents and U/Th ratios are found from Greece (Foscolos et al., 1989) and Kangal, Sivas,Turkey (Karayigit et al., 2001) (Fig. 12II). Uranium enrichment in coal is attributed to the leaching of this element from the surrounding volcanic rocks (Foscolos et al., 1989; Dai et al., 2003).

The Nb/Ta ratio of lignites from WGD varies from 4.23 to 21.8, 12.5 on average, which are basically close to that of upper continental crust (Taylor and McLennan, 1985), the sandstones from WGD, lignites from Hongqi Coal Mine, Kangal (Karayigit et al., 2001), and Beypazari (Querol et al., 1997), and Ge-bearing lignite from Luzanovka of GDRFE (Seredin, 2006) (Fig. 12III), but distinctly lower than that (average ratio of 27 lignite samples is up to 459) of the Ge-bearing lignites from LGD (Qi and Hu, 2002; Qi et al., 2004).

4.6. A possible source and genetic model for WGD

Although the coal basin is surrounded by Quaternary basalts, Hercynian diorite and granodiorite, and Late Jurassic granite (Fig. 1), the following facts exclude the possibility of basalt as the source rock: (1) the emplacement of basalt (Quaternary) is later than the formation of Shenli Coalfield (Early Cretaceous), (2) detrital W-bearing minerals, which usually formed in mineralized veins in granites, were identified in the lignite of WGD (Zhuang et al., 2006; Fig. 7), (3) of the high field strength elements, Nb and Ta show a conservative or least-mobile geochemicial behavior in weathering process (Taylor and McLennan, 1985; Nesbitt and Markovics, 1997), as well as the coal-forming process of the No.6-1 coal seam (Appendix III), indicating Nb/Ta ratio can be used to evaluate provenance. The average value of Nb/Ta ratios of lignite (12.5, Table 1) and the overlying sandstone (11.0, Table 1) are close to that of granite and upper continental crust (12 and 11.4, respectively), instead of that (17) of basalt (Taylor and McLennan, 1985; Dostal and Chatterjee, 2000), and (4) there is a clear correlation between the trace element geochemistry of the basement rocks and that of the overlying Ge-bearing coals (Seredin and Danilcheva, 2001).

Germanium deposits overlying granite basement are distinctly enriched in Sb, Ge, W, As, Be, U, Cs and Tl (Seredin and Danilcheva, 2001; Qi and Hu, 2002). These elements are generally enriched in the lignite or sandstone from WGD. All these facts indicate that most trace elements in the coal seam of WGD possibly derived from a granitic source or the diorite, granodiorite, or granite, peripherally distributed in the south part outside of Shengli Coalfield.

It should be noted that: (1) WGD distributed on the margin of a large coal-bearing basin, Shengli Coalfield (Fig. 1); (2) Ge contents of the No.6-1 coal seam of WGD shows a fan-shaped decreasing trend from the Southeast to the Northwest; (3) the gradient of Ge content is very steep at the margin of the coal seam; (4) Ge can be enriched in different (upper, middle and lower) proportion of the No.6-1 coal seam and Ge profiles showed a sharp variation within a small area, and (5) the faults destroyed the continuous distribution of the No.6-1 coal seam with the Ge-mineralized coal mainly distributed between the two faults. These geological features of WGD are quite different from those of LGD and GDRFE. The latter two are generally situated in small depressions, and Ge deposits, which consist of several ore bodies, equant or elongated, along faults, configurations. The ore bodies of LGD and GDRFE are usually situated at fault intersection. Ge mainly concentrated in the top or bottom of coal seams and Ge-mineralized coal seams are usually close to the granite in the basement of LGD and GDRFE (Seredin and Danilcheva, 2001; Qi et al., 2004). High epigenetic mineralization of Au–Pt group elements (PGE, up to a few ppm) at the brown coal of Pavlovsk in GDRFE (Seredin, 2004) also distinguished the normal content (<50 ng/g) of PGE–Au at the lignite of WGD (Zhuang et al., 2006).

The enrichment of Ge in lignite of LGD and GDRFE was generally attributed to ascending Ge-rich hydrothermal solution, which circulated in the fault system and leached abundant Ge from the granite in the basement and transported them into coal-bearing basin where Ge had been fixed by organic matter during diagenesis (Seredin and Danilcheva, 2001; Qi et al., 2004). The enrichment of Ge in coal seam near surface and a fan-shaped decreased trend of Ge from the southeast to the northwest of the No.6-1 coal seam in WGD argue for a lateral transferred Ge-rich solution, which may be derived from the leaching of granitoids in the southern part. Furthermore, the uneven distribution of Ge in the No.6-1 coal seam (Fig. 3) excludes the possibility of a syn-sedimentary fixation process of Ge by organic matter. It is difficult to imagine that this uneven distribution of Ge was caused by the fluctuation of water within such a small area during the coal forming process. Moreover, no distinct hydrothermal sediments (such as the hydrothermal sedimentary siliceous rock in LGD; Qi et al., 2004) have been found in the WGD lignite, indicating that the No.6-1 coal seam was formed in a normal sedimentary environment without hydrothermal solutions. The controlling effect of temperature on the solubility of tetrahedral GeO_2 (Pokrovski and Schott, 1998) determined that the low temperature solutions could not transport abundant Ge. For example, the concentrations of Ge in seawater and river waters are 0.05–0.10 ppb, distinctly lower than those (1–40 ppb Ge) of geothermal waters from Japan or Iceland (Arnórsson, 1984). This also may be the reason why the lignite in the hanging wall of F_2 fault only contains 0.5 to 2.8 ppm Ge on the whole coal basis.

Du et al. (2004) and Zhuang et al. (2006) argued that, in epigenetic processes, Ge should be concentrated at the top or bottom of a coal seam, obeying 'Zilbermints Law' (Yudovich, 2003), instead of in the middle proportion of coal seam. If the following factors were

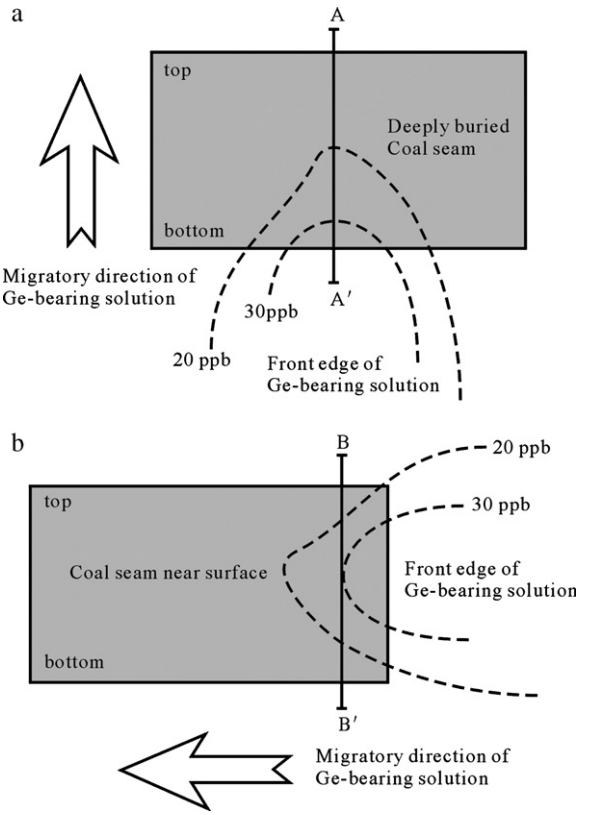

Fig. 13. Sketched maps show relationships between migratory direction of Ge-bearing solution, width of front edge of Ge-bearing solution, and Ge profile in two typical circumstances.

taken into accounts, the distribution of Ge in No. 6-1 coal seam of WGD would be easier to explain. These factors include the thickness of coal seam, depth of burial of coal seam, ground water level, migratory direction of Ge-bearing solution, and the width of front edge of Ge-bearing solution. Two typical circumstances are simplified and illustrated in Fig. 13. For a deeply buried thick coal seam in a confined water system, when the ascending Ge-bearing solution penetrated the coal seam, the bottom of A–A′ profile will preferentially concentrate more abundant Ge than the middle and top (Fig. 13a). However, when a laterally transferred Ge-rich solution reached a thick coal seam near surface, depending on the relative ratio of thickness of coal seam and the width of front edge of Ge-bearing solution and the angle of Ge-bearing solution entered coal seam, the middle proportion of B–B′ profile may preferentially concentrate more abundant Ge (Fig. 13b).

5. Conclusions

(1) The lignite samples of WGD are distinctly enriched in Be, Ge, Sb, W, and U, and depleted in Rb, Nb, Sn, and Ta, compared with the average composition of upper continental crust. The average values of Be, Ge, Sb, W, and U also are higher than those of overlying sandstone of WGD and the Ge-barren lignite of Hongqi Coal Mine, as well as the average concentration of elements in the USA coals and worldwide coals.

(2) Four groups of elements may be classified according to the mode of occurrence in coal: Ge–Mo, Tl–Ga–Zn–Co, Rb–Cs, and W–U–Cd–Y–Pb–Cu–Hf–Zr–Th–Sn–Nb–Ta–Ti–Sb–Ba–Sr–Mn–Be associations. The first association contains elements with negative correlation coefficients with ash yield, and they show mainly organic affinity. The last three associations contain elements with negative to high correlation coefficients with ash yield, mainly associated with sulfide or aluminosilicate minerals. Silver-bearing particles or native silver were identified by SEM-EDX in the lignites from WGD and Hongqi Coal Mine.

(3) Ge and Mo are concentrated in different proportion of coal seam in different sections, while the rest elements more or less follow the distribution of ash yield. TiO_2-normalized elemental profiles reveal that the ratios of Be/TiO_2, Ge/TiO_2, W/TiO_2, U/TiO_2, Mo/TiO_2, Sb/TiO_2, Tl/TiO_2, and Sr/TiO_2 of the lignite samples of WGD are much higher than the reference ratios of sandstone from WGD and lignite from Hongqi Coal Mine, many (more than 90%) of these elements (Be, Ge, W, U, Mo, Sb, Tl, and Sr) may be transported into coal seam by solution.

(4) Most trace elements in the Ge-bearing lignite of WGD may have been derived from a granitic source, and the enrichment of Be, Ge, Sb, W, U may be attributed to an epigenetic lateral transferred Ge-bearing solution that leached these elements form the granitic source and transported them into the lignite, where these elements were fixed.

Acknowledgement

Natural Sciences Foundation of China financially supported this project (Grant No. 40302018). We would like to thank Tongli Ge Refine Co., Ltd., Xilingol, Inner Mongolia for their support during field sampling, Associate Professor XianglinTu in Guangzhou Institute of Geochemistry, Chinese Academy of Sciences, and Associate Professor Xiuming Liu in the Institute of Geochemistry, Chinese Academy of Sciences, for the assistance during ICP-MS and SEM-EDX experiments. This paper benefited largely from the reviews and suggestions of Dr. Shifeng Dai, James C. Hower, and an unknown reviewer.

Appendix A. Supplementary material

Supplementary data associated with this article can be found, in the online version, at doi:10.1016/j.coal.2006.08.005.

References

Arnórsson, S., 1984. Germanium in Icelandic geochermal systems. Geochimica et Cosmochimica Acta 48, 2489–2502.

Bernstein, L.R., 1985. Germanium geochemistry and mineralogy. Geochimica et Cosmochimica Acta 49, 2409–2422.

Bilali, L.E., Rasmussen, P.E., Hall, G.E., Fortin, D., 2002. Role of sediment composition in trace metal distribution in lake sediments. Applied Geochemistry 17, 1171–1181.

Bouška, V., 1981. Geochemistry of Coal. Academia, Prague, pp. 164–216.

Brown, R.D., 2000. Germanium. U.S. Geological Survey Minerals Yearbook—2000, pp. 33.1–33.3.

Dai, S.F., Ren, D.Y., Hou, X.Q., Shao, L.Y., 2003. Geochemical and mineralogical anomalies of the late Permian coal in the Zhijin coalfield of southwest China and their volcanic origin. International Journal of Coal Geology 55, 117–138.

Dai, S.F., Ren, D.Y., Tang, Y.G., Yue, M., Hao, L.M., 2005. Concentration and distribution of elements in Late Permian coals from western Guizhou Province, China. International Journal of Coal Geology 61, 119–137.

Dostal, J., Chatterjee, A.K., 2000. Contrasting behaviour of Nb/Ta and Zr/Hf ratios in a peraluminous granitic pluton (Nova Scotia, Canada). Chemical Geology 163, 207–218.

Du, G., Tang, D.Z., Wu, W., Sun, P.C., Bai, Y.L., Xuan, Y.Q., Huang, G.J., 2003. Preliminary discussion on genetic geochemistry of paragenetic germanium deposit in Shenli Coalfield, Inner Mongolia. Geoscience 17 (4), 453–458 (in Chinese with English abstract).

Du, G., Tang, D.Z., Wu, W., Sun, P.C., Bai, Y.L., Yang, W.B., Xuan, Y.Q., Zhang, L.C., 2004. Research on grade variation regularity of paragenetic germanium deposit along uprightness in Shengli Coalfield, Inner Mongolia. Coal Geology & Exploration 32 (1), 1–4 (in Chinese with English abstract).

Dypvik, H., Harris, N.B., 2001. Geochemical facies analysis of fine-grained siliciclastics using Th/U, Zr/Rb and (Zr+Rb)/Sr ratios. Chemical Geology 181, 131–146.

Finkelman, R.B., 1993. Trace and minor elements in coal. In: Engel, M.H., Macko, S.A. (Eds.), Organic Geochemistry. Plenum, New York, pp. 593–607.

Finkelman, R.B., Bostick, N.H., Dulong, F.T., Senftle, F.E., Thorpe, A.N., 1998. Influence of an igneous intrusion on the inorganic geochemistry of a bituminous coal from Pitkin County, Colorado. International Journal of Coal Geology 36, 223–241.

Foscolos, A.E., Goodarzi, F., Koukouzas, C.N., Hatziyannis, G., 1989. Reconnaissance study of mineral matter and trace elements in Greek lignites. Chemical Geology 76, 107–130.

Fralick, P.W., Kronberg, B.I., 1997. Geochemical discrimination of clastic sedimentary rock sources. Sedimentary Geology 113, 111–124.

Gobeil, C., Macdonald, R.W., Smith, J.N., 1999. Mercury profiles in sediments of the Arctic Ocean basins. Environmental Science & Technology 33, 4194–4198.

Goodarzi, F., 1988. Elemental distribution in coal seams at the fording coal mine, British Columbia, Canada. Chemical Geology 68, 129–154.

Hower, J.C., Ruppert, L.F., Eble, C.F., 1999. Lanthanide, yttrium, and zirconium anomalies in the Fire Clay coal bed, Eastern Kentucky. International Journal of Coal Geology 39, 141–153.

Hower, J.C., Ruppert, L.F., Williams, D.A., 2002. Controls on boron and germanium distribution in the low-sulfur Amos coal bed, Western Kentucky coalfield, USA. International Journal of Coal Geology 53, 27–42.

Ilger, J.D., Ilger, W.A., Zingaro, R.A., Mohan, M.S., 1987. Modes of occurrence of uranium in carbonaceous uranium deposits: characterization of uranium in a South Texas (U.S.A.) lignite. Chemical Geology 63, 197–216.

Karayigit, A.I., Gayer, R.A., Ortac, F.E., Goldsmith, S., 2002. Trace elements in the Lower Pliocene fossiliferous Kangal lignites, Sivas, Turkey. International Journal of Coal Geology 47, 173–189.

Krotenski, J., Sotirov, A., 2002. Trace and major element content and distribution in Neogene lignite from the Sofia Basin, Bulgaria. International Journal of Coal Geology 52, 63–82.

Magenheim, A.J., Gieskes, J.M., 1992. Hydrothermal discharge and alteration in near-surface sediments from the Guaymas Basin, Gulf of California. Geochimica et Cosmochimica Acta 56, 2329–2338.

Nesbitt, H.W., Markovics, G., 1997. Weathering of granodioritic crust, long-term storage of elements in weathering profiles, and petrogenesis of siliclastic sediments. Geochimica et Cosmochimica Acta 61, 1653–1670.

Pokrovski, G.S., Schott, J.A., 1998. Experimental study of the complexation of silicon and germanium with aqueous organic species: implications for germanium and silicon transport and Ge/Si ratio in natural waters. Geochimica et Cosmochimica Acta 62, 3413–3428.

Qi, H.W., Hu, R.Z., 2002. Trace element geochemistry of Lincang Germanium Deposit. Coal Geology & Exploration 30 (2), 1–2 (in Chinese with English abstract).

Qi, H.W., Hu, R.Z., Su, W.C., Qi, L., Feng, J.Y., 2004. Continental hydrothermal sedimentary siliceous rock and genesis of superlarge germanium (Ge) deposit hosted in coal: a study from the Lincang Ge deposit, Yunnan, China. Sciences in China Series D Earth Sciences 47, 973–984.

Qing, S.L., 2001. Preservative principals of germanium deposit in Shengli Coal-field of Inner Mongolia and prospecting direction. Coal Geology of China 13 (3), 18–19 (in Chinese with English abstract).

Querol, X., Whateley, M.K.G., Fernández-Turiel, J.L., Tuncali, E., 1997. Geological controls on the mineralogy and geochemistry of the Beypazari lignite, central Anatolia, Turkey. International Journal of Coal Geology 33, 255–271.

Rasmussen, P.E., Villard, D.J., Gardner, H.D., Fortescue, J.A.C., Schiff, S.L., Shilts, W.W., 1998. Mercury in lake sediments of the Precambrian Shield near Huntsville, Ontario, Canada. Environmental Geology 33, 170–181.

Ren, D.Y., Zhao, F.H., Wang, Y.Q., Yang, S.J., 1999. Distribution of minor and trace elements in Chinese coals. International Journal of Coal Geology 40, 109–118.

Seredin, V.V., 2003. Anomalous concentrations of trace elements in the Spetsugli Germanium Deposit (Paclovka brown coal deposit, Southern Promorye): communication 2. Rubidium and cesium. Lithology and Mineral Resources 38, 233–241.

Seredin, V.V., 2004. The Au–PGE mineralization at the Pavlovsk Brown Coal Deposit, Primorye. Geology of Ore Deposits 46 (1), 36–63.

Seredin, V.V., 2006. Ge-bearing coals of the Luzanovka Graben, Pavlovka Brown Coal Deposit, Southern Promorye. Lithology and Mineral Resources 41, 280–301.

Seredin, V.V., Danilcheva, J., 2001. Coal-hosted Ge deposits of the Russian far east. In: Piestrynsky, A., et al. (Eds.), Mineral Deposits at the Beginning of the 21st Century. Swets & Zeitlinger Publishers, Lisse, The Netherlands, pp. 89–92.

Smimov, V.I., 1977. Ore Deposits of the USSR, vol. III. Pifman Publ., London, pp. 455–462.

Sturz, A.A., Sturdivant, A.E., Leif, R.N., Simoneit, B.R.T., Gieskes, J.M., 1996. Evidence for retrograde hydrothermal reactions in near surface sediments of Guaymas Basin, Gulf of California. Applied Geochemistry 11, 645–665.

Taylor, S.R., 1965. The application of trace element data to problems in petrology. In: Ahrens, L.A., Press, F., Runcorn, S.K., Urey, C. (Eds.), Physical and Chemical of the Earth, vol. 6. Pergamon, pp. 135–213.

Taylor, S.R., McLennan, S.M., 1985. The continental crust: its composition and evolution. Blackwell Scientific Publications, Oxford, pp. 9–67.

Valkovic, V., 1983. Trace Elements in Coal, vol. 1. CRC Press, pp. 133–138.

Wang, L.M., 1999. Introduction of the geological feature and explorating of Wulantuga germanium deposit in Xilinguole League, Inner Mongolia. Geology of Inner Mongolia 3, 15–20 (in Chinese with English abstract).

Weber, J.N., 1973. Geochemistry of Germanium. Dowden, Hutchingon and Ross, Inc., Stroudsburg, Pennsylvania, pp. 424–434.

Weiss, D., Shotyk, W., Rieley, J., Page, S., Gloor, M., Reese, S., Mattinez-Cortizas, A., 2002. The geochemistry of major and selected trace elements in a forested peat bog, Kalimantan, SE Asia, and its implications for past atmospheric dust deposition. Geochimica et Cosmochimica Acta 66, 2307–2323.

Yudovich, Y.E., 2003. Notes on the marginal enrichment of Germanium in coal beds. International Journal of Coal Geology 56, 223–232.

Zhao, J.Y., Tang, X.Y., Huang, W.H., 2002. Abundance of trace elements in coal of China. Coal Geology of China 14, 5–13 (Suppl in Chinese with English abstract).

Zhuang, H.P., Lu, J.L., Fu, J.M., Liu, J.Z., 1998. Lincang superlarge germanium deposit in Yunnan province, China: sedimentation, diagenesis, hydrothermal process and mineralization. Journal of China University of Geosciences 9, 129–136.

Zhuang, X.G., Querol, X., Alastuey, A., Juan, R., Plana, F., Soler, A.L., Du, G., Martynov, V.V., 2006. Geochemistry and mineralogy of the Cretaceous Wulantuga high-germanium coal deposit in Shengli coal field, Inner Mongolia, Northeastern China. International Journal of Coal Geology 66, 119–136.